Origins of robustness in translational control via eukaryotic translation initiation factor (eIF) 2

Mohammad Farhan Khan [1], Sarah Spurgeon [3#] and Tobias von der Haar [2#]

[1] School of Engineering and Digital Arts and [2] School of Biosciences, University of Kent, Canterbury, UK; and [3] Department of Electronic and Electrical Engineering, University College London, London, UK

[#] For correspondence: s.spurgeon@ucl.ac.uk or t.von-der-haar@kent.ac.uk

Abstract

Phosphorylation of eukaryotic translation initiation factor 2 (eIF2) is one of the best studied and most widely used means for regulating protein synthesis activity in eukaryotic cells. This pathway regulates protein synthesis in response to stresses, viral infections, and nutrient depletion, among others. We present analyses of an ordinary differential equation-based model of this pathway, which aim to identify its principal robustness-conferring features. Our analyses indicate that robustness is a distributed property, rather than arising from the properties of any one individual pathway species. However, robustness-conferring properties are unevenly distributed between the different species, and we identify a guanine nucleotide dissociation inhibitor (GDI) complex as a species that likely contributes strongly to the robustness of the pathway. Our analyses make further predictions on the dynamic response to different types of kinases that impinge on eIF2.

Introduction

mRNA translation is an important controller of gene expression levels. Together with transcriptional regulation, it quantitatively determines protein expression from any given gene (Hershey et al., 2007) . Translation occurs in distinct stages termed initiation, elongation, termination and recycling. While regulation of both initiation and elongation can be used to control gene expression levels (Chu et al., 2014) , translation initiation is thought to be the stage predominantly targeted for such control (Gebauer and Hentze, 2004) .

In eukaryotes, translation initiation involves attachment of the small ribosomal subunit to the mRNA 5'-end, followed by movement along the 5'-UTR or "scanning". This movement is arrested when a start codon is recognized (Hinnebusch, 2014) , at which point the large ribosomal subunit joins the small subunit and the elongation stage begins.

All events within translation initiation are controlled by translation initiation factors, proteins or protein complexes that associate with mRNAs and ribosomal subunits (Hinnebusch, 2014) . Many initiation factors are subject to control via signaling pathways that adapt gene expression to particular internal or external states, like growth conditions or developmental programs.

One of the best studied translational control mechanisms impinges on the eukaryotic initiation factor 2 (eIF2). eIF2 forms ternary complexes (TCs) which involve its three protein subunits, the initiator tRNA, and guanine nucleotides. In the GTP-bound form, TCs form 43S-preinitiation complexes with small ribosomal subunits and a host of other initiation factors. In 43S complexes, eIF2 structurally supports contacts of the initiator tRNA with the ribosomal A-site, as well as having functional roles by communicating to the ribosome the presence or absence of a start codon in the A-site. When a start codon in a sufficiently favourable sequence context enters the ribosomal A-site during scanning, hydrolysis of the eIF2-bound GTP to GDP is induced through conformational changes which are relayed from the ribosomal subunit to eIF2, and this is instrumental for arresting the scanning process.

eIF2 eventually leaves the complex in a GDP-bound form, and needs to undergo guanine nucleotide exchange from the GDP-to the GTP-bound form before it is competent for the next round of translation initiation. *In vivo*, this exchange reaction requires the presence of a guanine nucleotide exchange factor (GEF) termed eIF2B (Mohammed-Qureshi et al., 2008; Wortham and Proud, 2015), and is further regulated by a guanine nucleotide dissociation inhibitor (GDI) function of eIF5, another 43S complex member (Jennings and Pavitt, 2010) .

eIF2 is subject to regulation via phosphorylation at multiple sites, most importantly at serine 51 in its alpha subunit (Price et al., 1991) . Phosphorylation at this residue converts eIF2 from a substrate of eIF2B to its competitive inhibitor, thereby disrupting the guanosine exchange cycle required to sustain ongoing translation (Matts et al., 1983) . Because eIF2B is usually present in substoichiometric amounts compared to eIF2 (Jedlicka and Panniers, 1991; von der Haar and McCarthy, 2002) , even partial phosphorylation of

eIF2 can quantitatively block gene expression.

Various kinases are known to phosphorylate eIF2 (Donnelly et al., 2013) . A highly conserved kinase is Gcn2 which is activated by uncharged tRNAs (Dong et al., 2000), thereby using products of translational activity as an input for its regulation, a classical example of a feedback loop. Gcn2 is unusual in that it is a single-substrate kinase, that is to say, Gcn2 has no other known targets besides eIF2. Another eIF2 kinase, PERK, is activated by the accumulation of unfolded proteins in the endoplasmic reticulum (ER), similarly connecting an output of translational activity to its regulation in a feedback loop. Other types of kinase are known that regulate eIF2 through regulatory inputs that are not derived from translational activity. Such kinases include PKR, which is activated by double-stranded RNA (a hallmark of viral infection), and HRI, which links synthesis of globins to the amount of heme present in erythroid precursors (Chen, 2006). Between them, the eIF2 kinases are essential for the adaptation to numerous stresses, the execution of developmental programs, and the avoidance of disease states.

Due to decades of work, the molecular biology of the regulatory pathways involving eIF2 are now understood in good detail. In contrast, the dynamic behaviour of the eIF2-related systems is much less well understood. Several groups have begun to use computational and mathematical analyses to study dynamic aspects of eIF2-dependent regulation, either in the context of the overall translation initiation pathway (Dimelow and Wilkinson, 2009; Spirin, 2009) or by focusing specifically on the eIF2-related reactions (El-Haroun et al., 2010; Manchester, 1990; You et al., 2010). The main focus of these studies has been the proof of concept that modelling of the complex molecular systems in question is feasible, and to establish quantitative relationships between different activities involved in translation initiation and its control. These studies have yielded interesting insights into translational regulation by eIF2, but they typically address the paucity of experimental information on reaction rates by extensive parameter fitting, and there is uncertainty over how well fitted parameters relate to real parameters *in vivo*.

The number and types of eIF2 kinases differs strongly between organisms, comprising eg only Gcn2 in baker's yeast; Gcn2 and HRI in fission yeast; and Gcn2, PKR, Perk and HRI in human cells (Zhan et al., 2004). Moreover, even structurally highly conserved reactions such as the eIF2B-catalysed guanosine exchange can occur with rate constants that differ by orders of magnitude in differing organisms (Nika et al., 2000). Despite these substantial differences, the ways in which eIF2-dependent translational control is used appears fundamentally similar in different organisms. In addition to reaction rates, the structure of the regulatory pathways in question may therefore be defining pathway features. Accordingly, we focus our attention on the pathway structure and its relation to features such as robust regulation, rather than on relatively uncertain reaction rates obtained by parameter fitting.

The cellular pathways involving eIF2 can be considered as molecular switches that connect specific inputs (eg nutrient levels) to specific translational activity states. Switches of this kind display characteristics like robustness (ie to not switch unless there is an appropriate input that requires the switch to operate) and sensitivity (ie to reliably switch upon receiving the appropriate stimulus). In the present study, we explicitly

consider translational control via phosphorylation of eIF2 as a molecular switch, and use tools from the control engineering domain to study how the molecular architecture of this switch determines its switching properties.

Results and Discussion

Model implementation and parameterisation

As basis for our analyses of eIF2-dependent translational control, we established a mathematical model representing all elements required for translational control via eIF2. The model was established *de novo* based on the most recent descriptions of relevant reactions in the literature, as described in the introduction section.

Similar to other published models investigating translational control (Dimelow and Wilkinson, 2009; You et al., 2010), our model is based on a system of ordinary differential equations. We consider all reactions that connect the eIF2:GDP:eIF5 complex which is released from the ribosome following completion of translation initiation (Singh et al., 2006) with the eIF2:GTP complex, which is the starting point for a new round of ternary complex formation and translation initiation. The corresponding network of reactions constitutes the reactions of "core" pathways in figure 1. In order to not unnecessarily increase the dimensionality of the model, we represented the many other reactions in the physiological translation initiation pathway as a simple sink for eIF2:GTP and eIF5 and a stoichiometric source for eIF2:GDP, without further biochemical detail (figure 1). This approach, which distinguishes ours from other published models, enables us to use translation as a tunable black box which consumes eIF2:GTP and eIF5 with the correct rates, without requiring in depth modelling of the many reactions that connect eIF2:GTP to the formation of an elongation-competent ribosome.

Recent findings suggest that the pathways for the regeneration of eIF2:GDP can follow two routes in principle, and these are both represented in our model for the first time. eIF2 is released from the translation initiation process most likely as an eIF2:GDP:eIF5 complex (Singh et al., 2006) . Formation of the eIF2:GDP:eIF2B GEF complex can either occur via release of eIF5 prior to recruitment of eIF2B (termed route 1 in figure 1 and in the following), or via formation of an intermediate complex comprising both eIF2B and eIF5 (route 2). Recent results on the functions of eIF2B as an activator of eIF5 dissociation from eIF2:GDP:eIF5 complexes (Jennings et al., 2016, 2013) indicate that route 2 is likely preferred, this is discussed in further detail below.

In addition to the core pathways, our model contains a number of reactions that represent the regulation of translation via phosphorylation of eIF2. In implementing these reactions, we reduced the complexity of the various kinases and phosphatases acting on eIF2 to their fundamental, underpinning principles. We introduce a generic kinase (K) that can be activated by binding to a kinase activator (KA), which reflects real-world molecules like Gcn2 and tRNA, or PKR and dsRNA. We do not explicitly consider the molecular details of the activation mechanisms, such as the autophosphorylation step involved in activation of Gcn2.

The kinase:activator complex is competent for phosphorylation of eIF2:GDP, which in its phosphorylated form interacts with eIF2B to form a catalytically inactive guanine nucleotide exchange complex . We allow eIF2 to be dephosphorylated by a generic phosphatase reaction (R11), which in our model operates with a constant background rate.

We model kinase activation in two modes, either in a situation in which KA is injected into the system from an external source, or where KA is generated as part of the translation reaction (the distinction between these scenarios is discussed in more detail below). The latter mode requires the introduction of two additional reactions, R12 and R13, into the model although in the majority of our analyses these reactions are absent. The full ODE system representing the model (including R12 and R13) is given in supplementary file 1. For simulations, this model was run using the modified Rosenbrock solver from Matlab (ode23 (Shampine and Reichelt, 1997)).

Although we aimed to model the regulation via eIF2 based on generic features conserved throughout eukaryotic evolution, we needed to constrain the abundance of molecular species of the model using physiologically realistic values. We used biochemical data generated with baker's yeast for this purpose (table 1), as this is the organism with the most comprehensive literature on this topic. To complement the incomplete parameter set, we used a procedure based on the standard Levenberg-Marquardt (LM) parameter fitting algorithm (Moré, 1978) . As a constraint for this algorithm, we set a target translation rate equivalent to 13,000 proteins per cell per second as previously estimated for a haploid yeast cell (von der Haar, 2008).

The parameter fitting exercise yielded a combination of rate constants that allowed the model to achieve non-zero steady states when run in the absence of kinase activator (KA). In some cases, data are available either for the modelled reactions or for biochemically similar reactions, allowing us to judge physiological relevance of the modelled rate constants (table 2). Several of the reactions are very close in our model to measured rates, including GDP release from eIF2:eIF2B (R6), eIF2 dephosphorylation (R11) and the removal of uncharged tRNA (R13). Other apparent model rates differ somewhat from measured rates (eg complex formation between eIF2 and eIF2B, R3, or phosphorylation of eIF2, R9), while still being entirely within physiologically possible bounds. For the majority of the reactions involved in formation of macromolecular complexes, we have no direct experimental comparisons available, although all reported rate constants are at least theoretically possible. With all of these comparisons, one must keep in mind that rates which are not rate limiting for the flux through model may not actually be constrained, and that in these cases we would expect a parameter fitting algorithm to return a random rate compatible with the target flux through the pathway. Overall, we take the good fit between modelled and measured rate constants as an indication that our model recapitulates a number of biological properties of the pathway.

Biological observations indicate that translation has low response coefficients for changes in the levels of eIF2, eIF2B and eIF5 (Firczuk et al., 2013), as well as being generally robust to mutation-induced changes in rate constants in these reactions (Asano et al., 1999; Richardson et al., 2004). We wished to evaluate in

how far this robustness was reflected in our model, by evaluating in how far flux through reaction R7/R1 (which approximates translational activity, figure 1) was robust to perturbations in other model parameters.

The robustness criterion was initially evaluated by randomly varying rate constants within the scheme over a +/- 50% window, and recording corresponding changes in translational activity. Figure 2 illustrates this for both steady-state translation without a kinase-activating stress (figure 2 A) and in the case of a kinase-activating stress applied at t = 0 s (figure 2B). Steady-state translation under non-stress conditions in our model captures the robustness of real-life translation against parameter changes, and translation can be maintained in the face of all tested parameter perturbations within +/- 10 % of the target steady state. Upon activation of the eIF2 kinase, translational activity drops to zero within 4-6 minutes. eIF2 kinase-dependent regulation of the system will be explored further below.

Origins of robustness in eIF2-dependent regulation

In the previous sections we demonstrated that our model shares defining features with physiological translation systems, including robustness to perturbations. From a biological point of view, such robustness is a critical prerequisite for the functioning of molecular circuits that are subject to random internal fluctuations, as well as being affected by unpredictable changes in the cellular environment. Robustness is also a desirable feature in most technological control systems. This has motivated the development of mathematical tools in the engineering domain for investigating robustness-determining features of such systems. In the following section, we explore the use of such tools for the analysis of robustness in the eIF2-dependent translational control pathways.

In our initial analyses, the impact of varying individual rate constants by +/-50% had no major impact on the robustness of the system. Although analysing the robustness of the model by varying individual rate constants between the limits of +/-50% has biological significance, knowing the extreme limits to which individual rate constants can vary without impacting the robustness of the system may be useful as well. The model of eIF2-dependent regulation is both non-linear and high-dimensional. The analysis of such systems may be difficult, and standard tools for analysing robustness in very general classes of non-linear systems are not available. For this reason, control analyses frequently start by generating appropriate linearized representations to replicate the behaviour of the non-linear model over a given range of the state-space.

We used this approach to assess the robustness of the eIF2 reaction network under non-stress conditions, by linearizing the model including reactions R1 to R11 (ie without the feedback reactions R12 and R13, figure 1) with both the concentration and rate of change of the kinase activator KA set to zero. Details of the mathematical procedure are described in the “Model and Methods” section below.

The linearized model was subjected to an analysis approach known as structured singular value (μ) analysis (Kim et al., 2006), which evaluates the limits of robustness of a pathway against a single parametric

perturbation. Within control engineering, robust stability is a measure of how much uncertainty of a specific parameter the feedback loop can tolerate before becoming unstable. The structured singular value, or μ, is the mathematical tool used to compute this robust stability margin. Figure 3 shows the upper bound of μ where the inverse of the peak value determines the maximum value of the perturbation in a single parameter which has no impact on the robust stability of the system. From figure 3, the maximum allowable percentage variation of an individual rate constant *k* which will not affect the robust stability of the model is 7.95×10^{5} %. This high percentage value reinforces the very high robustness of the eIF2 pathway to perturbations in individual rate constants, and indicates that robustness to a large extent the result of its structure, rather than of specific sets of rate constants with which the system operates.

In addition to the μ analysis which characterises the robustness of the overall system, we applied a model reduction technique to the linear model, which essentially analyses the effect of the dynamics of individual species on the observed input-output behaviour. In this way, the influence of particular species on the output of interest can be quantified. We then compared the behaviour of the full non-linear model to the behaviour of derived models in which the dynamics of individual species are constrained (the latter are termed truncated models).

Figure 4 displays the results of this analysis via Bode magnitude plots. The salient information on the effect of constraining the dynamics of individual species is in the comparison of the lines representing each model. Removing the dynamics of a species which does not affect the input-output behaviour of the model at all would result in perfect tracking of these lines. Deviation demonstrates the degree to which the input-output behaviour is dependent upon the dynamics which have been removed.

The results of this analysis are illustrated for three representative species in figure 4. The selection of species shown in this figure spans the full range of effects observed also for other species of the model. In all cases, removal of individual species resulted in good tracking of the frequency response of the original and reduced model in some frequency ranges, whereas in other frequency ranges imperfect tracking was observed. However, the frequency range over which tracking was observed clearly differed between the model species. This indicates that robustness determining features are generally distributed between the species of the model, but that the dynamics of some species makes a greater contribution to the robustness of the system than others. The greatest contribution in this respect appears to come from the dynamics of the eIF2:eIF2B:eIF5:GDP species, whereas the smallest contribution is made by the dynamics of the eIF2:GDP species.

To test these findings and explore the usefulness of the analysis based on the linear model, we eliminated the dynamics of the core species in turn from the original non-linear model and compared the corresponding output with that obtained from the original non-linear model. Note that to determine the impact of individual species on the general translational rate, the rate of change of the species is set to zero and a corresponding steady-state condition is imposed on the dynamics. This reduces the order of the model. Eliminating the dynamics of the three core species illustrated in figure 4 from the full, linear model

has no effect on the ability of the model to reach a steady state. Moreover, the steady state output of the reduced models is within less than 0.1% of the steady state of the full, non-reduced model (differing by 0.045%, 0.022% and 0.021% for eIF5:eIF2B:eIF2:GDP, eIF2B:eIF2:GDP, and eIF2:GDP, respectively). As predicted from the linear analysis, the nonlinear simulations results demonstrate that removing the dynamics of eIF5:eIF2B:eIF2:GDP produces the most effect on the output behaviour whilst removal of eIF2:GDP has a least substantial effect, although in all cases the effects on the steady state are small.

The role of redundant pathways for formation of the guanosine exchange complex

The recent discovery that eIF5 functions as a guanine nucleotide dissociation inhibitor (GDI) as well as a GTPase activator protein (GAP) for eIF2, and the ensuing characterisation of an eIF2:GDP:eIF5:eIF2B intermediate complex, suggest that there are two independent pathways for formation of the guanosine exchange complex eIF2:GDP:eIF2B. Visual inspection of the model structure coupled with observations from the control analysis of the model suggests that the system might be operable in principle via each of the two parallel pathways in isolation, ie either by disallowing formation of the eIF2:GDP:eIF5:eIF2B complex via R3 and R4 (figure 1) and only allowing the eIF2:GDP:eIF2B complex to form via R2 and R3, or by disallowing R2 and R3, and only allowing formation of the eIF2:GDP:eIF2B complex via R4 and R5.

To test whether the system could run stably via either of the two branches alone, we compared model runs where both the abundance of the species in one of the branches and the rate constants for the respective reactions were set to zero, with the rest of the model parameterised with identical rate constants as for the full model. This is the modelling equivalent of introducing a mutation in a binding site that completely abrogates the formation of the respective complex. We observed that a model in which formation of the eIF5-containing eIF2:eIF2B complex was disallowed reached a steady state that was only slightly (<5%) lower than the steady state of the full model (figure 5A). Similarly, when kinase activator was added, translational activity decayed to zero with very similar dynamics whether or not reactions R4 and R5 were allowed (figure 5B). This behaviour mimics the redundancy that is frequently built in to engineering systems to ensure failure in one path does not cause system failure.

Interestingly, eIF5 mutants with reduced affinity for eIF2 and reduced GDI activity, where the flux of molecules should be strongly redirected towards route 1, have been shown to allow growth at almost normal rates (Jennings 2010). However, the same mutants did not respond normally to Gcn2 activation, contrary to our model predictions. The authors of this study postulated that the inability of Gcn2 to appropriately regulate translation relied on a fine balance between levels of eIF2 phosphorylation and eIF2B availability, which may not be reflected in our model with sufficient accuracy.

Surprisingly, when reactions R2 and R3 were disallowed, the model could not adopt a steady state. These observations suggest that of the two pathways connecting eIF2:GDP:eIF5, the one proceeding via the eIF2:GDP:eIF5:eIF2B complex is not essential for the principal operability of the pathway. However, as the analyses in figure 4 suggest, the dynamics of this pathway do play roles in determining the robustness of translational control mechanisms against perturbations.

Translational regulation by eIF2 kinases

The preceding sections considered the influence of various parameters, primarily on the non-stressed mode of the model (ie in the absence of kinase activator). We next turned our attention to the situation when kinase activators are present. Existing eIF2 kinases operate in two fundamentally different modes: their activating signal can either arise from the translational machinery itself, or from pathways unconnected to translation. Examples for the first case include Gcn2 which is activated when the consumption of charged tRNAs by translation exceeds the capacity of the tRNA synthetases to regenerate them, and PERK, which is activated when protein synthesis overwhelms the folding capacity of the ER. In these cases, regulation of the translational machinery is connected to a translational output in a classic feedback loop. Similar feedback loops have previously been analysed in other translational control pathways (Betney et al., 2012; de Silva et al., 2010), where feedback properties were found to contribute strongly to the overall dynamic behaviour of the pathway. Examples for the non-feedback mode include PKR, which is activated by viral RNA i.e. not by a product of the translational machinery.

It should be noted that in our analyses we consider modes of regulation where inactive kinase is activated by an activating molecule, which is the case for Gcn2 and PKR. Some eIF2 kinases are regulated in the opposite fashion, ie they are active in the apo-form but are inhibited by inhibiting molecules (such as heme in the case of HRI). Both the addition of an activator or the removal of an inhibitor cause fractional changes in the abundance of active kinase, and our analyses can be understood to illustrate either mode of regulation.

Because non-feedback regulation is the simpler case, we start our analyses with this scenario. For this purpose, we add a species KA (kinase activator) to the model that interacts with the eIF2 kinase with a macromolecular equilibrium binding constant of 10 μM to form an active kinase complex, which is then competent to phosphorylate eIF2.

If we allow the model to run at equilibrium and then raise the concentration of KA, we observe that the translation rate drops to zero over time. The rate of response is concentration dependent, with a lower threshold for the response time (arbitrarily defined here as the time after which translation has dropped by 99%) between two and three minutes (figure 6A). The exact details of the response curve are dependent on the exact rate parameters chosen for kinase activation and eIF2 phosphorylation, but the observed response time is close to the behaviour observed in yeast and mammalian cells.

To model feedback regulation by kinases which rely on activation via translation products, we introduced two new reactions (R12 and R13 in figure 1) into the model which mimic the production of a kinase activator like uncharged tRNA by the translational machinery, and the removal of this activator from the system (representing eg re-charging of uncharged tRNAs by the tRNA synthetases). The behaviour of the system is then principally determined by the ratio of production to removal of the kinase activator: for very low ratios, the system operates essentially as it does in the absence of kinase activator (the top line in the

graph in figure 6B represents a system producing kinase activator at 1/1000th of its rate of removal, and has a steady state indistinguishable from a model running in the absence of kinase activator). For higher ratios, the system very quickly becomes strongly responsive to the production of kinase activator. Under the parameter combinations shown in figure 6, this happens even when the rate of production of KA is much lower than the rate of removal: this is because under steady state conditions, some free tRNA accumulates and is stabilised by forming a complex with the kinase even at low KA production and high removal rates, and this is sufficient to activate eIF2 phosphorylation. Exactly how responsive the system is depends on a number of parameters including the ratio of the rate constants with which the kinase activator interacts with the kinase activator removal system and with the kinase (eg, the association rates of tRNAs with tRNA synthetases and Gcn2), the stability of the kinase:activator complex, and the ratio of phosphorylation and dephosphorylation rates for eIF2. One of the consequences of the strong responsiveness of our model to production of kinase activator is that there is only a very narrow window of parameter combinations in which the system adopts a non-zero steady state: even for low rates of production of kinase activator, the system tends towards a zero translation rate, albeit approaching this rate over very different time scales depending on the rate with which kinase activator is produced. The very strong sensitivity to kinase activity in both the fed-back and non fed-back modes may be caused by the high molar excess of eIF2 over eIF2B (Singh et al., 2007; von der Haar and McCarthy, 2002), which means that eIF2B can be inhibited even when eIF2 is only partially phosphorylated. It is interesting to consider in how far these observed features of our model reflect the real world behaviour of eIF2-dependent translational control. Real-world systems contain a number of control elements that are absent from our model. For example, Gcn2 itself can be phosphorylated by TORC1, and this phosphorylation prevents activation of Gcn2 kinase activity (Cherkasova and Hinnebusch, 2003). TORC1 activity also has a stimulating effect on translational activity. In consequence, when high translational activity is required, the sensitive system would be prevented from being inappropriately activated eg by low levels of tRNAs. Similarly, PKR can be inhibited by trans-acting modulators like p58^{IPK} (Barber et al., 1994), which could similarly be used to attenuate the response to activation of the kinase. If the strong responsiveness our model predicts is indeed a real-world feature of eIF2-mediated translational control, this could explain why additional regulators evolved for these kinases, and the combination of strong response and trans-acting modulators would ensure both high robustness and high sensitivity of translational control.

Conclusions

Our computational investigation into robustness determining features of translational regulation impinging on eIF2 formulates a number of experimentally testable hypotheses.

The model recapitulates biological control in a number of aspects. The model can reach a steady state translational activity at levels very similar to a well-studied *in vivo* system (yeast), upon activation of the eIF2 kinase translation ceases on a time-sale of minutes, and both of these properties are robust with

respect to parameter choices. We find indications of strong robustness using different analysis approaches, namely explicit parameter variation and structured singular value analyses. This finding of strong robustness is validated by experimental observations that translation *in vivo* can operate despite relatively severe parameter perturbations resulting eg from mutations in eIF2 and eIF2B (Asano et al., 1999; Richardson et al., 2004).

Our further analyses based on model derivatives where dynamics of individual species are constrained indicate that this strong robustness results from distributed model features, and cannot be traced to the behaviour of a single individual species. However, some species' dynamics contribute more to the robustness of the system than others. A strongly contributing species in this respect is the eIF2:eIF2B:eIF5 complex which, although our analyses predict it to be non-essential for the basic operability of the system (figure 5), show the strongest changes in robustness when its dynamics are constrained (figure 4). Interestingly, Jennings *et al.* very recently characterised an eIF2 mutant that prevents eIF5 from functioning as a GDI (Jennings et al., 2016) . This mutant allows normal growth rates, but does not allow robust regulation of translational activity under conditions which would normally lead to activation of the Gcn2 kinase. Although this study did not directly evaluate the effect of the eIF2 mutant on the eIF2:eIF2B:eIF5 complex, these findings are consistent with our predictions that normal formation of this complex is important for robust regulation, but not essential for the basic operability of translation.

One of the outcomes from our study is an indication where models of translational control via eIF2 could be improved in future. There is a paucity of rate constants available for formation of the different macromolecular complexes. This introduces a high degree of freedom into the parameter estimation process, which could be reduced if accurate, experimentally measured rates were available. Moreover, new aspects of the modelled pathways are still being uncovered, such a the recent discovery of a "fail-safe" mechanism by which eIF2 phosphorylation potentiates translational response to eIF2 kinase activation (Jennings et al., 2017). Considering these new findings in model-based analyses will require introducing new reactions and rate-constants, which will only be feasible if the need for parameter fitting can be reduced for existing parameters.

Given the strong sensitivity of our current model to kinase activation, it is likely that additional regulatory layers such as the priming of GCN2 by TOR or the regulation of PKR by trans-acting cellular regulators like $p58^{IPK}$ could strongly modulate the dynamics with which translation responds to regulatory input. The inclusion of such regulation in the model would clearly be desirable, although it is likely that this would introduce too many degrees of freedom in simple, ODE-based models as the majority of these interactions are dynamically almost completely uncharacterised. Qualitative approaches such as Petri-Net based models (Chaouiya, 2007) may enable the analysis of such wider regulatory networks without explicitly considering rate constants.

Methods

Model simulations

The full ODE system representing the model (including R12 and R13) is given in supplementary file 1. For simulations, this model was run using the modified Rosenbrock solver from Matlab (ode23 (Shampine and Reichelt, 1997)).

Levenberg-Marquardt implementation

The rate constants of the model have been estimated using the Levenberg-Marquardt (LM) algorithm (Marquardt, 1963) . In order to develop a naturally behaving mathematical model, the rate constants are optimised using the LM algorithm integrated with pathway characteristics such as positivity and robustness analysis.

Using the LM algorithm alone to parameterise computational models may result in uncertain combinations of parameter values, which may not follow experimental observations appropriately. Therefore, to overcome the limitation of parameter uncertainty, we integrated the robustness characteristics of the general translation rate (Y_1) to parameter changes within the LM algorithm. The integrated parameterisation process used in this work is discussed below. Note that for simplicity the concentration of species considered in the eIF2-dependent translational regulation model are denoted by Y (a conversion from Y notation to standard molecular biology notation is given in table 3).

In order to quantify the changes in general translation rate due to variation in the rate constant vector *k*, the following equation is used.

$$\xi_1 = |Y_{1D} - Y_1(Y_i(0), k_i, t)| \quad (1)$$

where, ξ_1 is an absolute error between *in-vitro* and *in-silico* experimental values, Y_{1D} is the *in-vitro* experimental data value of the general translation rate in a yeast cell, $Y_1(Y(0),k, t)$ is the *in-silico* experimental value of the general translation rate obtained after solving the ODEs using the modified Rosenbrock solver with $Y(0)$ and k initial conditions. After obtaining different combinations of parameter values giving $\xi_2 \equiv 0$, the value for each combination of k is perturbed +/-50% from the original value and the error ξ_2 with respect to Y_{1D} is recorded. The average value of normalised absolute error ξ_2 can be determined from (2),

X (2)

where, T is the evaluation time and Δk is equal to +/-50% of the original k value. The purpose of perturbing the rate constants is to analyse the robustness of general translation rate. Hence a lower value of ξ_2 defines high robustness against internal parametric changes.

Note that, to cope with the limitation that concentration values of most of the species/complexes are unknown, we have opted for a random selection approach which adopts a random value of the initial concentration that should lie within yeast molecular concentration. Typically, in yeast cells the molecular concentrations lie approximately between 10nM-10µM. Hence, the initial concentration of remaining

species/complexes are randomly varied in a bounded limit of [10^{-3},10] µM in a way that the target constraints can be achieved (refer to the subsection on model implementation and parameterisation).

Model linearisation

In control theory, the non-linear model can be linearised around an equilibrium point to investigate some of its properties such as robust stability etc. Linearisation simplifies the non-linear interaction of the species, so that the individual effect of the rate constants can be investigated. There are some limitations of the linear approximation of non-linear systems, that is the linear system is an approximation that is only valid across small regions around equilibrium point. Therefore the approximate linear system accurately predicts the local behaviour of the non-linear systems instead of global.

A generalised form of the non-linear mathematical model given in supplementary file 1 (excluding R12 and R13) can be defined as follows:

$$\acute{Y}(t) = \acute{f}(Y(t), k) \quad (3)$$

where, *Y* is the non-negative concentration of the species, *t* is the evaluation time and *k* is a rate constant vector. In order to find the equilibrium point of a model or a steady state value of all the species, eq. 3 is to be solved by equating it to zero. Note that, substituting *f*(*Y*(*t*); *k*) to zero implies no change in the state of all species as time progresses that is all species have attained a steady state. Solving the equation results into one of the biologically feasible equilibrium point Y^{eq} displayed in table 3.

Prior to investigating the role of uncharged tRNA (Y_{13}) on other species, it is beneficial to eliminate the dynamics of Y_{13} from the original non-linear model. The investigation has revealed that Y_{13} has attained the quasi steady state or constant steady state value for varying initial concentrations (Segel and Slemrod, 1989). Hence, substituting $Y_{13} = 0$ makes no difference in the behaviour of modified non-linear system compared to the original non-linear system. Performing this task gives freedom to consider Y_{13} as an applied input *u* and helps to analyse the direct impact of uncharged tRNA on translation rate. The state space model of the modified non-linear model can be defined as follows:

$$\begin{aligned} \acute{Y}(t) &= Y(Y(t), k) + B\big(Y(t)\big)u \\ Z(t) &= Y_1(t) \end{aligned} \quad (4)$$

where vector $B\big(Y(t)\big) = \big[00000000 - k_{8f}Y_9 k_{8f}Y_9 000\big]^T$, vector $Y(t) = [Y_1 Y_2 \cdots Y_{12} Y_{14}]^T$, vector $k = \big[k_1 k_{2f} k_{2r} \cdots k_{12}\big]$, $u = Y_{13}$ and $Z(t)$ is the output signal or translation rate. The state space representation of an approximate LTI model of a modified non-linear system around the equilibrium point can be re-written in the form:

$$\begin{aligned} \acute{Y} &= AY + Bu \\ Z &= DY \end{aligned} \quad (5)$$

where *A* is a constant Jacobian matrix, *B* and *D* are the constant input and output vectors respectively given as:

$$B = [00000000 - 4.331 \times 10^{-11} 4.331 \times 10^{-11} 000]$$

$$D = [1000000000000]$$

Note that the matrix *A* of dimensions 13×13 is a function of the equilibrium point and rate constant vector *k*. The Jacobian matrix *A* represents the behaviour of the overall biological system around an equilibrium point (Y^{eq}).

Mu (μ) analysis

Within control engineering, robust stability is a measure of how much uncertainty of a specific parameter the feedback loop can tolerate before becoming unstable. In order to determine the extreme limits to which rate constants of the model can vary without impacting the robustness of the system, we conducted a structured singular value (μ) analysis (Fan et al., 1991; Kim et al., 2006).

$$\mu = \frac{1}{\min_{\Delta}\{\acute{\sigma}(\Delta) \vee det(I - M(s)\Delta) = 0 for \Delta \in B_{\Delta}\}} \quad (6)$$

where $\acute{\sigma}$ represents the maximum singular value, *M*(s) denotes the transfer function of the system and B_{Δ} represents a set of uncertainties **Δ**. From the above equation it is clear that the principle at which μ-analysis works is finding the smallest value of $\acute{\sigma}(\Delta)$ that can make $I - M(s)\Delta$ singular, and when there is no **Δ** such that $det(I - M(s)\Delta) = 0$ then $\mu = 0$.

Note that, μ-analysis is a deterministic measure which computes a level of uncertainty at which the model is guaranteed to produce desirable results. One of the advantage of opting μ-analysis is that it provides information on robustness of the system when the parameters of the system encounters simultaneous perturbation (Kim et al., 2006). This particular scenario resembles the actual behaviour of robust biological systems because under environmental disturbances the parameters of the biological systems can fluctuate simultaneously without impacting the behaviour of the system. So higher value of upper bound of μ^{-1} is desirable for robust biological systems.

In order to evaluate the parametric perturbation limits of a biological system, the equivalent linearised biological system needs to be connected through a feedback control loop to a matrix of uncertain parameters **Δ**. The robustness analysis of a biological system using μ requires the system to be represented in a stable linear time invariant (LTI) form.

To analyse the robustness of the system, a parametric uncertainty matrix block **Δ** is introduced into the LTI biological system represented in (5). Note that, the parametric uncertainty matrix block is only consisting of diagonal entries of the individual parameters. Thus, obtaining upper bound of μ-analysis it can be guaranteed that the system is robust provided that no single parameter differs more than upper bound of μ^{-1}×100% from its nominal value. Figure 7 represents the biological system *M*(*s*) connected through a closed feedback loop which can be destabilised from the smallest possible uncertainty **Δ**. Note that, $\Delta = diag\left[\delta_{k1}\delta_{k2f}\delta_{k2r}\cdots\delta_{k12}\right]$ and *M*(*s*) is the transfer function of the LTI model defined as:

$M(s) = D(sI - A_i)^{-1}B_i$	(7)

Now, introducing **Δ** into the system changes the rate constant *k* to $k(1+\delta_k)$. The state space representation of the perturbed system is as follows:

$\delta\acute{Y} = a\delta Y + B_0\Delta Y$ $Y = D_0\delta Y$	(8)

Note that the dimensions of the constant matrices B_0 and D_0 are 13×20 and 20×13 respectively. The matrices B_0 and D_0 for the perturbed LTI system are defined below.

$B_0(i,j) = 1$	(9)

for (*i,j*) equals (1,11), (2,1), (2,3), (2,7), (3,3), (3,9), (3,10), (3,17), (4,2), (4,5), (5,4), (5,6), (6,4), (6,8), (7,6), (7,9), (7,15), (7,18), (8,10), (9,13), (10,12), (10,15), (10,19), (11,17), (11,19), (12,16), and (13,14).

$B_0(i,j) = -1$	(10)

for (*i,j*) equals (1,1), (1,20), (2,2), (2,6), (3,2), (3,8), (3,16), (4,3), (4,4), (5,5), (5,7), (5,11), (6,5), (6,9), (6,10), (7,7), (7,8), (7,14), (8,11), (9,12), (10,13), (10,14), (11,16), (11,18), (12,17), (13,15), and (13,19). The remaining elements of $B_0(i,j) = 0$. On the other hand, all the elements of matrix D_0 are zero except:

$D_0(1,1) = k_1,\ D_0(2,2) = k_{4f}Y_3^{eq},\ D_0(2,3) = k_{4f}Y_2^{eq}, D_0(3,4) = k_{4r}, D_0(4,4) = k_{5f}, D_0(5,5) = k_{5r}Y_6^{eq}, D_0(5,6) = k_{5r}Y_5^{eq}, D_0(6,2) = k_{2f}, D_0(7,5) = k_{2r}Y_7^{eq}, D_0(7,7) = k_{2r}Y_5^{eq}, D_0(8,3) = k_{3f}Y_7^{eq}, D_0(8,7) = k_{3f}Y_3^{eq}, D_0(9,6) = k_{3r}, D_0(10,6) = k_6, D_0(11,5) = k_7Y_8^{eq}, D_0(11,8) = k_7Y_5^{eq}, D_0(12,9) = k_{8f}Y_{13}^{eq}, D_0(13,10) = k_{8r}, D_0(14,7) = k_{9af}Y_{10}^{eq}, D_0(14,10) = k_{9af}Y_7^{eq}, D_0(15,13) = k_{9ar}, D_0(16,3) = k_{10f}Y_{11}^{eq}, D_0(16,11) = k_{10f}Y_3^{eq}, D_0(17,12) = k_{10r}, D_0(18,11) = k_{11}, D_0(19,13) = k_{9b}, D_0(20,1) = k_{12}$	(11)

Analysing system (8) using the Matlab μ-analysis tool within the Robust Control Toolbox from Mathworks, will give the value at which the rate constant can be perturbed individually without impacting the structured robustness of the system.

References

Asano, K., Krishnamoorthy, T., Phan, L., Pavitt, G.D., Hinnebusch, A.G., 1999. Conserved bipartite motifs in yeast eIF5 and eIF2Bepsilon , GTPase-activating and GDP-GTP exchange factors in translation initiation, mediate binding to their common substrate eIF2. EMBO J. 18, 1673–1688. https://doi.org/10.1093/emboj/18.6.1673

Barber, G.N., Thompson, S., Lee, T.A.E.G., Strom, T.E.D., Jagust, R., Darveau, A., Katze, M.G., 1994. The 58-kilodalton inhibitor of the interferon-induced double-stranded RNA-activated protein kinase is a tetratricopeptide repeat

protein with oncogenic properties. Proc. Natl. Acad. Sci. USA 91, 4278–4282.

Betney, R., de Silva, E., Mertens, C., Knox, Y., Krishnan, J., Stansfield, I., 2012. Regulation of release factor expression using a translational negative feedback loop: a systems analysis. RNA 18, 2320–2334. https://doi.org/10.1261/rna.035113.112

Chaouiya, C., 2007. Petri net modelling of biological networks. Brief. Bioinform. 8, 210–219. https://doi.org/10.1093/bib/bbm029

Chen, J.-J., 2006. Regulation of protein synthesis by the heme-regulated eIF2 kinase: relevance to anemias. Blood 109, 2693–9. https://doi.org/10.1182/blood-2006-08-041830

Cherkasova, V.A., Hinnebusch, A.G., 2003. Translational control by TOR and TAP42 through dephosphorylation of eIF2alpha kinase GCN2. Genes Dev. 17, 859–872. https://doi.org/10.1101/gad.1069003

Chu, D., Barnes, D.J., Von Der Haar, T., 2011. The role of tRNA and ribosome competition in coupling the expression of different mRNAs in Saccharomyces cerevisiae. Nucleic Acids Res. 39, 6705–6714. https://doi.org/10.1093/nar/gkr300

Chu, D., Kazana, E., Bellanger, N., Singh, T., Tuite, M.F., von der Haar, T., 2014. Translation elongation can control translation initiation on eukaryotic mRNAs. EMBO J. 33, 21–34. https://doi.org/10.1002/embj.201385651

de Silva, E., Krishnan, J., Betney, R., Stansfield, I., 2010. A mathematical modelling framework for elucidating the role of feedback control in translation termination. J. Theor. Biol. 264, 808–21. https://doi.org/10.1016/j.jtbi.2010.01.015

Dey, M., Trieselmann, B., Locke, E.G., Lu, J., Cao, C., Dar, A.C., Krishnamoorthy, T., Dong, J., Sicheri, F., Dever, T.E., 2005. PKR and GCN2 Kinases and Guanine Nucleotide Exchange Factor Eukaryotic Translation Initiation Factor 2B (eIF2B) Recognize Overlapping Surfaces on eIF2. Mol. Cell. Biol. 25, 3063–3075. https://doi.org/10.1128/MCB.25.8.3063-3075.2005

Dimelow, R.J., Wilkinson, S.J., 2009. Control of translation initiation: a model-based analysis from limited experimental data. J. R. Soc. Interface 6, 51–61. https://doi.org/10.1098/rsif.2008.0221

Dong, J., Qiu, H., Garcia-Barrio, M., Anderson, J., Hinnebusch, a G., 2000. Uncharged tRNA activates GCN2 by displacing the protein kinase moiety from a bipartite tRNA-binding domain. Mol. Cell 6, 269–279. https://doi.org/10.1016/S1097-2765(00)00028-9

Donnelly, N., Gorman, A.M., Gupta, S., Samali, A., 2013. The eIF2α kinases: Their structures and functions. Cell. Mol. Life Sci. 70, 3493–3511. https://doi.org/10.1007/s00018-012-1252-6

El-Haroun, E.R., Bureau, D.P., Cant, J.P., 2010. A mechanistic model of nutritional control of protein synthesis in animal tissues. J. Theor. Biol. 262, 361–9. https://doi.org/10.1016/j.jtbi.2009.09.034

Fan, M.K.H., Tits, A.L., Doyle, J.C., 1991. Robustness in the presence of mixed parametric uncertainty and unmodeled dynamics. IEEE Trans. Automat. Contr. 36, 25–38. https://doi.org/10.1109/9.62265

Firczuk, H., Kannambath, S., Pahle, J., Claydon, A., Beynon, R., Duncan, J., Westerhoff, H., Mendes, P., McCarthy, J.E., 2013. An in vivo control map for the eukaryotic mRNA translation machinery. Mol. Syst. Biol. 9, 1–13. https://doi.org/10.1038/msb.2012.73

Fjeld, C.C., Denu, J.M., 1999. Kinetic analysis of human serine/threonine protein phosphatase 2Calpha. J. Biol. Chem. 274, 20336–20343.

Gebauer, F., Hentze, M.W., 2004. Molecular mechanisms of translational control. Nat. Rev. Mol. Cell Biol. 5, 827–835. https://doi.org/10.1038/nrm1488

Hershey, J.W.B., Sonenberg, N., Mathews, M. (Eds.), 2007. Translational Control in Biology and Medicine, 3rd Ed. ed. Cold Spring Harbor Laboratory Press, Cold Spring Harbor, New York.

Hinnebusch, A.G., 2014. The scanning mechanism of eukaryotic translation initiation. Annu. Rev. Biochem. 83, 779–812. https://doi.org/10.1146/annurev-biochem-060713-035802

Jedlicka, P., Panniers, R., 1991. Mechanism of activation of protein synthesis initiation in mitogen- stimulated T lymphocytes. J Biol Chem 266, 15663–15669.

Jennings, M.D., Kershaw, C.J., Adomavicius, T., Pavitt, G.D., 2017. Fail-safe control of translation initiation by dissociation of eIF2α phosphorylated ternary complexes. Elife 6, e24542. https://doi.org/10.7554/eLife.24542

Jennings, M.D., Kershaw, C.J., White, C., Hoyle, D., Richardson, J.P., Costello, J.L., Donaldson, I.J., Zhou, Y., Pavitt, G.D., 2016. eIF2β is critical for eIF5-mediated GDP-dissociation inhibitor activity and translational control. Nucleic Acids Res. gkw657. https://doi.org/10.1093/nar/gkw657

Jennings, M.D., Pavitt, G.D., 2010. eIF5 has GDI activity necessary for translational control by eIF2 phosphorylation. Nature 465, 378–381. https://doi.org/10.1038/nature09003.eIF5

Jennings, M.D., Zhou, Y., Mohammad-Qureshi, S.S., Bennett, D., Pavitt, G.D., 2013. eIF2B promotes eIF5 dissociation from eIF2*GDP to facilitate guanine nucleotide exchange for translation initiation. Genes Dev. 27, 2696–2707. https://doi.org/10.1101/gad.231514.113

Kim, J., Bates, D.G., Postlethwaite, I., Ma, L., Iglesias, P.A., 2006. Robustness analysis of biochemical network models. IEE Proc. - Syst. Biol. 153, 96. https://doi.org/10.1049/ip-syb:20050024

Manchester, K.L., 1990. Kinetic modelling of the effect of alpha subunit phosphorylation on the activity of the protein synthesis initiation factor eIF-2. Biochem. Int. 22, 623–533.

Marquardt, D.W., 1963. An Algorithm for Least-Squares Estimation of Nonlinear Parameters. J. Soc. Ind. Appl. Math. 11, 431–441. https://doi.org/10.1137/0111030

Matts, R., Levin, D., London, I., 1983. Effect of phosphorylation of the alpha-subunit of eukaryotic initiation factor 2 on the function of reversing factor in the initiation of protein synthesis. Proc. Natl. Acad. Sci. U. S. A. 80, 2559–2563.

Mohammed-Qureshi, S.S., Jennings, M.D., Pavitt, G.D., 2008. Clues to the mechanism of action of eIF2B, the guanine-nucleotide-exchange factor for translation initiation. Biochem. Soc. Trans. 36, 658–664.

Moré, J.J., 1978. The Levenberg-Marquardt algorithm: Implementation and theory, in: Watson, G.A. (Ed.), Numerical Analysis: Proceedings of the Biennial Conference Held at Dundee, June 28–July 1, 1977. Springer Berlin Heidelberg, Berlin, Heidelberg, pp. 105–116. https://doi.org/10.1007/BFb0067700

Nika, J., Yang, W., Pavitt, G.D., Hinnebusch, A.G., Hannig, E.M., 2000. Purification and Kinetic Analysis of eIF2B from Saccharomyces cerevisiae. J. Biol. Chem. 275, 26011–26017. https://doi.org/10.1074/jbc.M003718200

Price, N.T., Welsh, G.I., Proud, C.G., 1991. Phosphorylation of only serine-51 in protein synthesis initiation factor-2 is associated with inhibition of peptide-chain initiation in reticulocyte lysates. Biochem. Biophys. Res. Commun. 176, 993–999. https://doi.org/10.1016/0006-291X(91)90380-P

Richardson, J.P., Mohammad, S.S., Pavitt, G.D., 2004. Mutations causing childhood ataxia with central nervous system hypomyelination reduce eukaryotic initiation factor 2B complex formation and activity. Mol. Cell. Biol. 24, 2352–2363.

Segel, L.A., Slemrod, M., 1989. The Quasi-Steady-State Assumption: A Case Study in Perturbation. SIAM Rev. 31, 446–477. https://doi.org/10.1137/1031091

Shampine, L.F., Reichelt, M.W., 1997. The MATLAB ODE Suite. SIAM J. Sci. Comput. 18, 1–22.

https://doi.org/10.1137/S1064827594276424

Singh, C.R., Lee, B., Udagawa, T., Mohammad-Qureshi, S.S., Yamamoto, Y., Pavitt, G.D., Asano, K., 2006. An eIF5/eIF2 complex antagonizes guanine nucleotide exchange by eIF2B during translation initiation. EMBO J. 25, 4537–4546. https://doi.org/10.1038/sj.emboj.7601339

Singh, C.R., Udagawa, T., Lee, B., Wassink, S., He, H., Yamamoto, Y., Anderson, J.T., Pavitt, G.D., Asano, K., 2007. Change in Nutritional Status Modulates the Abundance of Critical Pre-initiation Intermediate Complexes During Translation Initiation in Vivo. J. Mol. Biol. 370, 315–330. https://doi.org/10.1016/j.jmb.2007.04.034

Spirin, A.S., 2009. How Does a Scanning Ribosomal Particle Move along the 5′-Untranslated Region of Eukaryotic mRNA? Brownian Ratchet Model. Biochemistry 48, 10688–10692.

von der Haar, T., 2008. A quantitative estimation of the global translational activity in logarithmically growing yeast cells. BMC Syst. Biol. 2, 87. https://doi.org/10.1186/1752-0509-2-87

von der Haar, T., McCarthy, J.E.G., 2002. Intracellular translation initiation factor levels in Saccharomyces cerevisiae and their role in cap-complex function. Mol. Microbiol. 46, 531–544. https://doi.org/10.1046/j.1365-2958.2002.03172.x

Wortham, N.C., Proud, C.G., 2015. eIF2B: recent structural and functional insights into a key regulator of translation. Biochem. Soc. Trans. 43, 1234–40. https://doi.org/10.1042/BST20150164

You, T., Coghill, G.M., Brown, A.J.P., 2010. A quantitative model for mRNA translation in Saccharomyces cerevisiae. Yeast 27, 785–800. https://doi.org/10.1002/yea

Zhan, K., Narasimhan, J., Wek, R.C., 2004. Differential Activation of eIF2 Kinases in Response to Cellular Stresses in Schizosaccharomyces pombe. Genetics 1875, 1867–1875. https://doi.org/10.1534/genetics.104.031443

Table 1. Literature values used for model parameterisation.

Parameter	Value[a]	References
Translation	13,000 proteins per second	(von der Haar, 2008)
total cellular eIF2	18 µM	(Singh et al., 2007; von der Haar, 2008)
Total cellular eIF2B	1.8 µM	(Singh et al., 2007; von der Haar, 2008)
Total cellular eIF5	18 µM	(Singh et al., 2007)
Total cellular kinase (Gcn2)	0.09 µM	(Singh et al., 2007)

[a]Where appropriate, intracellular concentrations were calculated from molecule numbers based on a typical haploid yeast cell volume of 27 μm^3 or $2.7x10^{-14}$ litres (von der Haar and McCarthy, 2002) .

Table 2. Steady state rate constants and comparison to literature values.

Rate	Value	Reaction	Reported value
k1	1.77 s^{-1}	(translation)	A k1 value of **1.78 s^{-1}** is equivalent to a flux of ~13,000 translation events per second in the steady state (von der Haar, 2008)
k2f	7.59 s^{-1}	eIF5 release from 5:2:GDP	No data
k2r	0.91 $M^{-1}s^{-1}$		
k3f	6×10^{7} $M^{-1}s^{-1}$	2B:2:GDP complex formation	K_M of **0.7-1.2x10^{-8}** at 0˚C (Nika et al., 2000) vs. **2.5e^{-6}** calc. from (k6+k3r)/k3f
k3r	150 s^{-1}		
k4f	1.0 $M^{-1}s^{-1}$	5:2:2B:GDP complex formation	no data
k4r	0.72 s^{-1}		
k5f	0.36 s^{-1}	eIF5 release from 5:2:2B:GDP	no data
k5r	$1.6x10^{4}$ $M^{-1}s^{-1}$		
k6	0.72 s^{-1}	GDP release from 2:2B:GDP	**0.7-7 sec^{-1}** (Nika et al., 2000)
k7	$7.4x10^{4}$ $M^{-1}s^{-1}$	(translation)	A k7 value of **7.3x10^{4} M^{-1} s^{-1}** is equivalent to a flux of ~13,000 translation events per second in the steady state (von der Haar, 2008)
k8f	1×10^{6} $M^{-1}s^{-1}$	GCN2:tRNA complex formation	no data
k8r	203 s^{-1}		
k9af	1×10^{9} $M^{-1}s^{-1}$	phosphorylation reaction	K_M of **10^{-5} to 10^{-6} M** for human PKR (Dey et al., 2005) vs **1.0x10^{-4} M** calculated from (k9ar + k9b)/k9af
k9ar	167 s^{-1}		
k9b	1×10^{5} s^{-1}		
k10f	1×10^{2} $M^{-1}s^{-1}$	2-P:2B:GDP complex formation	no data
k10r	129 s^{-1}		
k11	1×10^{-4} s^{-1}	phosphatase reaction	**10^{-3} to 10^{-5} sec^{-1}** at 1 µM enzyme for human PP2Cα (Fjeld and Denu, 1999)
k12	1×10^{-8} s^{-1}	(tRNA release from translation)	na
k13	$1x10^{-2}$ s^{-1}	tRNA recharging	**10^{-2} to 10^{2} sec^{-1}** at 1-10 µM tRS for various yeast enzymes (Chu et al., 2011)

Table 3. Species denominations and equilibrium points for species abundance.

Y_1	translation	4.36×10^{-7} M
Y_2	eIF5:eIF2:GDP	1.19×10^{-7} M
Y_3	eIF2B	7.22×10^{-7} M
Y_4	eIF5:eIF2B:eIF2:GDP	1.78×10^{-7} M
Y_5	eIF5	1.11×10^{-5} M
Y_6	eIF2B:eIF2:GDP	1.07×10^{-6} M
Y_7	eIF2:GDP	3.74×10^{-7} M
Y_8	eIF2:GTP	9.44×10^{-6} M
Y_9	GCN2	4.33×10^{-17} M
Y_{10}	tRNA:GCN2	2.22×10^{-18} M
Y_{11}	eIF2-P	1.61×10^{-12} M
Y_{12}	eIF2-P:eIF2B	4.04×10^{-18} M
Y_{13}	tRNA	1.04×10^{-5} M
Y_{14}	tRNA:GCN2:eIF2	8.23×10^{-21} M

Figure Legends

Figure 1. Graphical presentation of the eIF2-dependent translational regulation model. The model is conceptually divided into a core section which comprises the reactions required for sustaining ongoing translation, and regulatory reactions that can be used to exert regulation on the core section. Regulation can be exerted either in a fed-back mode through reactions 12 and 13, or in a non-fed-back manner if reactions 12 and 13 are removed from the model. Double-headed arrows above the reaction numbers indicate reactions that are modelled via reversible mass-action kinetics. The species indicated are: 2, eIF2; 2-P, phosphorylated eIF2; 2B, eIF2B; 5, eIF5; K, kinase; KA, kinase activator.

Figure 2. Principal behaviour and robustness of the model. A, simulation of the model without kinase activator (KA in figure 1). **B,** simulation with 10 µM KA injected at t = 0 s. Error bars represent the variability of the model as observed in the parameter variation exercise discussed in the text.

Figure 3. Upper bound of the structured singular value µ. The inverse of the peak value determines the maximum value of the perturbation in a single parameter which has no impact on the robust stability of the system.

Figure 4. Bode diagrams for three representative model species. We observe partial tracking of the original and truncated, linearised models for all analysed species across the frequency range. The analysis indicates that eIF2:GDP can be expected to have the smallest effect on the input output behaviour of translational control via eIF2.

Figure 5. Model performance in the absence of redundant pathways leading to eIF2:eIF2B complex formation. When formation of the eIF2:GDP:eIF5:eIF2B intermediate complex is disallowed, the model shows a very similar steady-state in the absence of kinase activator (A) as well as a similar response to the presence of kinase activator (B). When formation of this complex is the only allowed route leading to the guanine nucleotide exchange complex (ie when decay of the eIF2:eIF5 complex into free eIF2:GDP and eIF5 is disallowed), the model does not reach a steady state.

Figure 6. eIF2 kinase-dependent regulation of translation. A, regulation in a non-fed-back model. Upon injection of kinase activator (KA) at t=0, translational activity declines with the rate of decline dependent on the concentration of the activator. The inset graph illustrates the time to reach a 99% reduction in translational activity as a function of KA concentration. B, regulation in a fed-back model. The evolution of the model starting without kinase activator is shown, as function of different production/removal ratios for KA.

645

Figure 7: *M*-Δ configuration of eIF2 pathway for μ analysis.

Origins of robustness in translational control via eukaryotic translation initiation factor (eIF) 2

Mohammad Farhan Khan [1], Sarah Spurgeon [3#] and Tobias von der Haar [2#]

[1] School of Engineering and Digital Arts and [2] School of Biosciences, University of Kent, Canterbury, UK; and [3] Department of Electronic and Electrical Engineering, University College London, London, UK

[#] For correspondence: s.spurgeon@ucl.ac.uk or t.von-der-haar@kent.ac.uk

Abstract

Phosphorylation of eukaryotic translation initiation factor 2 (eIF2) is one of the best studied and most widely used means for regulating protein synthesis activity in eukaryotic cells. This pathway regulates protein synthesis in response to stresses, viral infections, and nutrient depletion, among others. We present analyses of an ordinary differential equation-based model of this pathway, which aim to identify its principal robustness-conferring features. Our analyses indicate that robustness is a distributed property, rather than arising from the properties of any one individual pathway species. However, robustness-conferring properties are unevenly distributed between the different species, and we identify a guanine nucleotide dissociation inhibitor (GDI) complex as a species that likely contributes strongly to the robustness of the pathway. Our analyses make further predictions on the dynamic response to different types of kinases that impinge on eIF2.

Introduction

mRNA translation is an important controller of gene expression levels. Together with transcriptional regulation, it quantitatively determines protein expression from any given gene (Hershey et al., 2007) . Translation occurs in distinct stages termed initiation, elongation, termination and recycling. While regulation of both initiation and elongation can be used to control gene expression levels (Chu et al., 2014) , translation initiation is thought to be the stage predominantly targeted for such control (Gebauer and Hentze, 2004) .

In eukaryotes, translation initiation involves attachment of the small ribosomal subunit to the mRNA 5'-end, followed by movement along the 5'-UTR or "scanning". This movement is arrested when a start codon is recognized (Hinnebusch, 2014) , at which point the large ribosomal subunit joins the small subunit and the elongation stage begins.

All events within translation initiation are controlled by translation initiation factors, proteins or protein complexes that associate with mRNAs and ribosomal subunits (Hinnebusch, 2014) . Many initiation factors are subject to control via signaling pathways that adapt gene expression to particular internal or external states, like growth conditions or developmental programs.

One of the best studied translational control mechanisms impinges on the eukaryotic initiation factor 2 (eIF2). eIF2 forms ternary complexes (TCs) which involve its three protein subunits, the initiator tRNA, and guanine nucleotides. In the GTP-bound form, TCs form 43S-preinitiation complexes with small ribosomal subunits and a host of other initiation factors. In 43S complexes, eIF2 structurally supports contacts of the initiator tRNA with the ribosomal A-site, as well as having functional roles by communicating to the ribosome the presence or absence of a start codon in the A-site. When a start codon in a sufficiently favourable sequence context enters the ribosomal A-site during scanning, hydrolysis of the eIF2-bound GTP to GDP is induced through conformational changes which are relayed from the ribosomal subunit to eIF2, and this is instrumental for arresting the scanning process.

eIF2 eventually leaves the complex in a GDP-bound form, and needs to undergo guanine nucleotide exchange from the GDP-to the GTP-bound form before it is competent for the next round of translation initiation. *In vivo*, this exchange reaction requires the presence of a guanine nucleotide exchange factor (GEF) termed eIF2B (Mohammed-Qureshi et al., 2008; Wortham and Proud, 2015), and is further regulated by a guanine nucleotide dissociation inhibitor (GDI) function of eIF5, another 43S complex member (Jennings and Pavitt, 2010) .

eIF2 is subject to regulation via phosphorylation at multiple sites, most importantly at serine 51 in its alpha subunit (Price et al., 1991) . Phosphorylation at this residue converts eIF2 from a substrate of eIF2B to its competitive inhibitor, thereby disrupting the guanosine exchange cycle required to sustain ongoing translation (Matts et al., 1983) . Because eIF2B is usually present in substoichiometric amounts compared to eIF2 (Jedlicka and Panniers, 1991; von der Haar and McCarthy, 2002) , even partial phosphorylation of

eIF2 can quantitatively block gene expression.

Various kinases are known to phosphorylate eIF2 (Donnelly et al., 2013) . A highly conserved kinase is Gcn2 which is activated by uncharged tRNAs (Dong et al., 2000), thereby using products of translational activity as an input for its regulation, a classical example of a feedback loop. Gcn2 is unusual in that it is a single-substrate kinase, that is to say, Gcn2 has no other known targets besides eIF2. Another eIF2 kinase, PERK, is activated by the accumulation of unfolded proteins in the endoplasmic reticulum (ER), similarly connecting an output of translational activity to its regulation in a feedback loop. Other types of kinase are known that regulate eIF2 through regulatory inputs that are not derived from translational activity. Such kinases include PKR, which is activated by double-stranded RNA (a hallmark of viral infection), and HRI, which links synthesis of globins to the amount of heme present in erythroid precursors (Chen, 2006). Between them, the eIF2 kinases are essential for the adaptation to numerous stresses, the execution of developmental programs, and the avoidance of disease states.

Due to decades of work, the molecular biology of the regulatory pathways involving eIF2 are now understood in good detail. In contrast, the dynamic behaviour of the eIF2-related systems is much less well understood. Several groups have begun to use computational and mathematical analyses to study dynamic aspects of eIF2-dependent regulation, either in the context of the overall translation initiation pathway (Dimelow and Wilkinson, 2009; Spirin, 2009) or by focusing specifically on the eIF2-related reactions (El-Haroun et al., 2010; Manchester, 1990; You et al., 2010). The main focus of these studies has been the proof of concept that modelling of the complex molecular systems in question is feasible, and to establish quantitative relationships between different activities involved in translation initiation and its control. These studies have yielded interesting insights into translational regulation by eIF2, but they typically address the paucity of experimental information on reaction rates by extensive parameter fitting, and there is uncertainty over how well fitted parameters relate to real parameters *in vivo*.

The number and types of eIF2 kinases differs strongly between organisms, comprising eg only Gcn2 in baker's yeast; Gcn2 and HRI in fission yeast; and Gcn2, PKR, Perk and HRI in human cells (Zhan et al., 2004). Moreover, even structurally highly conserved reactions such as the eIF2B-catalysed guanosine exchange can occur with rate constants that differ by orders of magnitude in differing organisms (Nika et al., 2000). Despite these substantial differences, the ways in which eIF2-dependent translational control is used appears fundamentally similar in different organisms. In addition to reaction rates, the structure of the regulatory pathways in question may therefore be defining pathway features. Accordingly, we focus our attention on the pathway structure and its relation to features such as robust regulation, rather than on relatively uncertain reaction rates obtained by parameter fitting.

The cellular pathways involving eIF2 can be considered as molecular switches that connect specific inputs (eg nutrient levels) to specific translational activity states. Switches of this kind display characteristics like robustness (ie to not switch unless there is an appropriate input that requires the switch to operate) and sensitivity (ie to reliably switch upon receiving the appropriate stimulus). In the present study, we explicitly

consider translational control via phosphorylation of eIF2 as a molecular switch, and use tools from the control engineering domain to study how the molecular architecture of this switch determines its switching properties.

Results and Discussion

Model implementation and parameterisation

As basis for our analyses of eIF2-dependent translational control, we established a mathematical model representing all elements required for translational control via eIF2. The model was established *de novo* based on the most recent descriptions of relevant reactions in the literature, as described in the introduction section.

Similar to other published models investigating translational control (Dimelow and Wilkinson, 2009; You et al., 2010), our model is based on a system of ordinary differential equations. We consider all reactions that connect the eIF2:GDP:eIF5 complex which is released from the ribosome following completion of translation initiation (Singh et al., 2006) with the eIF2:GTP complex, which is the starting point for a new round of ternary complex formation and translation initiation. The corresponding network of reactions constitutes the reactions of "core" pathways in figure 1. In order to not unnecessarily increase the dimensionality of the model, we represented the many other reactions in the physiological translation initiation pathway as a simple sink for eIF2:GTP and eIF5 and a stoichiometric source for eIF2:GDP, without further biochemical detail (figure 1). This approach, which distinguishes ours from other published models, enables us to use translation as a tunable black box which consumes eIF2:GTP and eIF5 with the correct rates, without requiring in depth modelling of the many reactions that connect eIF2:GTP to the formation of an elongation-competent ribosome.

Recent findings suggest that the pathways for the regeneration of eIF2:GDP can follow two routes in principle, and these are both represented in our model for the first time. eIF2 is released from the translation initiation process most likely as an eIF2:GDP:eIF5 complex (Singh et al., 2006) . Formation of the eIF2:GDP:eIF2B GEF complex can either occur via release of eIF5 prior to recruitment of eIF2B (termed route 1 in figure 1 and in the following), or via formation of an intermediate complex comprising both eIF2B and eIF5 (route 2). Recent results on the functions of eIF2B as an activator of eIF5 dissociation from eIF2:GDP:eIF5 complexes (Jennings et al., 2016, 2013) indicate that route 2 is likely preferred, this is discussed in further detail below.

In addition to the core pathways, our model contains a number of reactions that represent the regulation of translation via phosphorylation of eIF2. In implementing these reactions, we reduced the complexity of the various kinases and phosphatases acting on eIF2 to their fundamental, underpinning principles. We introduce a generic kinase (K) that can be activated by binding to a kinase activator (KA), which reflects real-world molecules like Gcn2 and tRNA, or PKR and dsRNA. We do not explicitly consider the molecular details of the activation mechanisms, such as the autophosphorylation step involved in activation of Gcn2.

The kinase:activator complex is competent for phosphorylation of eIF2:GDP, which in its phosphorylated form interacts with eIF2B to form a catalytically inactive guanine nucleotide exchange complex . We allow eIF2 to be dephosphorylated by a generic phosphatase reaction (R11), which in our model operates with a constant background rate.

We model kinase activation in two modes, either in a situation in which KA is injected into the system from an external source, or where KA is generated as part of the translation reaction (the distinction between these scenarios is discussed in more detail below). The latter mode requires the introduction of two additional reactions, R12 and R13, into the model although in the majority of our analyses these reactions are absent. The full ODE system representing the model (including R12 and R13) is given in supplementary file 1. For simulations, this model was run using the modified Rosenbrock solver from Matlab (ode23 (Shampine and Reichelt, 1997)).

Although we aimed to model the regulation via eIF2 based on generic features conserved throughout eukaryotic evolution, we needed to constrain the abundance of molecular species of the model using physiologically realistic values. We used biochemical data generated with baker's yeast for this purpose (table 1), as this is the organism with the most comprehensive literature on this topic. To complement the incomplete parameter set, we used a procedure based on the standard Levenberg-Marquardt (LM) parameter fitting algorithm (Moré, 1978) . As a constraint for this algorithm, we set a target translation rate equivalent to 13,000 proteins per cell per second as previously estimated for a haploid yeast cell (von der Haar, 2008).

The parameter fitting exercise yielded a combination of rate constants that allowed the model to achieve non-zero steady states when run in the absence of kinase activator (KA). In some cases, data are available either for the modelled reactions or for biochemically similar reactions, allowing us to judge physiological relevance of the modelled rate constants (table 2). Several of the reactions are very close in our model to measured rates, including GDP release from eIF2:eIF2B (R6), eIF2 dephosphorylation (R11) and the removal of uncharged tRNA (R13). Other apparent model rates differ somewhat from measured rates (eg complex formation between eIF2 and eIF2B, R3, or phosphorylation of eIF2, R9), while still being entirely within physiologically possible bounds. For the majority of the reactions involved in formation of macromolecular complexes, we have no direct experimental comparisons available, although all reported rate constants are at least theoretically possible. With all of these comparisons, one must keep in mind that rates which are not rate limiting for the flux through model may not actually be constrained, and that in these cases we would expect a parameter fitting algorithm to return a random rate compatible with the target flux through the pathway. Overall, we take the good fit between modelled and measured rate constants as an indication that our model recapitulates a number of biological properties of the pathway.

Biological observations indicate that translation has low response coefficients for changes in the levels of eIF2, eIF2B and eIF5 (Firczuk et al., 2013), as well as being generally robust to mutation-induced changes in rate constants in these reactions (Asano et al., 1999; Richardson et al., 2004). We wished to evaluate in

how far this robustness was reflected in our model, by evaluating in how far flux through reaction R7/R1 (which approximates translational activity, figure 1) was robust to perturbations in other model parameters.

The robustness criterion was initially evaluated by randomly varying rate constants within the scheme over a +/- 50% window, and recording corresponding changes in translational activity. Figure 2 illustrates this for both steady-state translation without a kinase-activating stress (figure 2 A) and in the case of a kinase-activating stress applied at t = 0 s (figure 2B). Steady-state translation under non-stress conditions in our model captures the robustness of real-life translation against parameter changes, and translation can be maintained in the face of all tested parameter perturbations within +/- 10 % of the target steady state. Upon activation of the eIF2 kinase, translational activity drops to zero within 4-6 minutes. eIF2 kinase-dependent regulation of the system will be explored further below.

Origins of robustness in eIF2-dependent regulation

In the previous sections we demonstrated that our model shares defining features with physiological translation systems, including robustness to perturbations. From a biological point of view, such robustness is a critical prerequisite for the functioning of molecular circuits that are subject to random internal fluctuations, as well as being affected by unpredictable changes in the cellular environment. Robustness is also a desirable feature in most technological control systems. This has motivated the development of mathematical tools in the engineering domain for investigating robustness-determining features of such systems. In the following section, we explore the use of such tools for the analysis of robustness in the eIF2-dependent translational control pathways.

In our initial analyses, the impact of varying individual rate constants by +/-50% had no major impact on the robustness of the system. Although analysing the robustness of the model by varying individual rate constants between the limits of +/-50% has biological significance, knowing the extreme limits to which individual rate constants can vary without impacting the robustness of the system may be useful as well. The model of eIF2-dependent regulation is both non-linear and high-dimensional. The analysis of such systems may be difficult, and standard tools for analysing robustness in very general classes of non-linear systems are not available. For this reason, control analyses frequently start by generating appropriate linearized representations to replicate the behaviour of the non-linear model over a given range of the state-space.

We used this approach to assess the robustness of the eIF2 reaction network under non-stress conditions, by linearizing the model including reactions R1 to R11 (ie without the feedback reactions R12 and R13, figure 1) with both the concentration and rate of change of the kinase activator KA set to zero. Details of the mathematical procedure are described in the “Model and Methods” section below.

The linearized model was subjected to an analysis approach known as structured singular value (μ) analysis (Kim et al., 2006), which evaluates the limits of robustness of a pathway against a single parametric

perturbation. Within control engineering, robust stability is a measure of how much uncertainty of a specific parameter the feedback loop can tolerate before becoming unstable. The structured singular value, or μ, is the mathematical tool used to compute this robust stability margin. Figure 3 shows the upper bound of μ where the inverse of the peak value determines the maximum value of the perturbation in a single parameter which has no impact on the robust stability of the system. From figure 3, the maximum allowable percentage variation of an individual rate constant *k* which will not affect the robust stability of the model is 7.95×10^{5} %. This high percentage value reinforces the very high robustness of the eIF2 pathway to perturbations in individual rate constants, and indicates that robustness to a large extent the result of its structure, rather than of specific sets of rate constants with which the system operates.

In addition to the μ analysis which characterises the robustness of the overall system, we applied a model reduction technique to the linear model, which essentially analyses the effect of the dynamics of individual species on the observed input-output behaviour. In this way, the influence of particular species on the output of interest can be quantified. We then compared the behaviour of the full non-linear model to the behaviour of derived models in which the dynamics of individual species are constrained (the latter are termed truncated models).

Figure 4 displays the results of this analysis via Bode magnitude plots. The salient information on the effect of constraining the dynamics of individual species is in the comparison of the lines representing each model. Removing the dynamics of a species which does not affect the input-output behaviour of the model at all would result in perfect tracking of these lines. Deviation demonstrates the degree to which the input-output behaviour is dependent upon the dynamics which have been removed.

The results of this analysis are illustrated for three representative species in figure 4. The selection of species shown in this figure spans the full range of effects observed also for other species of the model. In all cases, removal of individual species resulted in good tracking of the frequency response of the original and reduced model in some frequency ranges, whereas in other frequency ranges imperfect tracking was observed. However, the frequency range over which tracking was observed clearly differed between the model species. This indicates that robustness determining features are generally distributed between the species of the model, but that the dynamics of some species makes a greater contribution to the robustness of the system than others. The greatest contribution in this respect appears to come from the dynamics of the eIF2:eIF2B:eIF5:GDP species, whereas the smallest contribution is made by the dynamics of the eIF2:GDP species.

To test these findings and explore the usefulness of the analysis based on the linear model, we eliminated the dynamics of the core species in turn from the original non-linear model and compared the corresponding output with that obtained from the original non-linear model. Note that to determine the impact of individual species on the general translational rate, the rate of change of the species is set to zero and a corresponding steady-state condition is imposed on the dynamics. This reduces the order of the model. Eliminating the dynamics of the three core species illustrated in figure 4 from the full, linear model

has no effect on the ability of the model to reach a steady state. Moreover, the steady state output of the reduced models is within less than 0.1% of the steady state of the full, non-reduced model (differing by 0.045%, 0.022% and 0.021% for eIF5:eIF2B:eIF2:GDP, eIF2B:eIF2:GDP, and eIF2:GDP, respectively). As predicted from the linear analysis, the nonlinear simulations results demonstrate that removing the dynamics of eIF5:eIF2B:eIF2:GDP produces the most effect on the output behaviour whilst removal of eIF2:GDP has a least substantial effect, although in all cases the effects on the steady state are small.

The role of redundant pathways for formation of the guanosine exchange complex

The recent discovery that eIF5 functions as a guanine nucleotide dissociation inhibitor (GDI) as well as a GTPase activator protein (GAP) for eIF2, and the ensuing characterisation of an eIF2:GDP:eIF5:eIF2B intermediate complex, suggest that there are two independent pathways for formation of the guanosine exchange complex eIF2:GDP:eIF2B. Visual inspection of the model structure coupled with observations from the control analysis of the model suggests that the system might be operable in principle via each of the two parallel pathways in isolation, ie either by disallowing formation of the eIF2:GDP:eIF5:eIF2B complex via R3 and R4 (figure 1) and only allowing the eIF2:GDP:eIF2B complex to form via R2 and R3, or by disallowing R2 and R3, and only allowing formation of the eIF2:GDP:eIF2B complex via R4 and R5.

To test whether the system could run stably via either of the two branches alone, we compared model runs where both the abundance of the species in one of the branches and the rate constants for the respective reactions were set to zero, with the rest of the model parameterised with identical rate constants as for the full model. This is the modelling equivalent of introducing a mutation in a binding site that completely abrogates the formation of the respective complex. We observed that a model in which formation of the eIF5-containing eIF2:eIF2B complex was disallowed reached a steady state that was only slightly (<5%) lower than the steady state of the full model (figure 5A). Similarly, when kinase activator was added, translational activity decayed to zero with very similar dynamics whether or not reactions R4 and R5 were allowed (figure 5B). This behaviour mimics the redundancy that is frequently built in to engineering systems to ensure failure in one path does not cause system failure.

Interestingly, eIF5 mutants with reduced affinity for eIF2 and reduced GDI activity, where the flux of molecules should be strongly redirected towards route 1, have been shown to allow growth at almost normal rates (Jennings 2010). However, the same mutants did not respond normally to Gcn2 activation, contrary to our model predictions. The authors of this study postulated that the inability of Gcn2 to appropriately regulate translation relied on a fine balance between levels of eIF2 phosphorylation and eIF2B availability, which may not be reflected in our model with sufficient accuracy.

Surprisingly, when reactions R2 and R3 were disallowed, the model could not adopt a steady state. These observations suggest that of the two pathways connecting eIF2:GDP:eIF5, the one proceeding via the eIF2:GDP:eIF5:eIF2B complex is not essential for the principal operability of the pathway. However, as the analyses in figure 4 suggest, the dynamics of this pathway do play roles in determining the robustness of translational control mechanisms against perturbations.

Translational regulation by eIF2 kinases

The preceding sections considered the influence of various parameters, primarily on the non-stressed mode of the model (ie in the absence of kinase activator). We next turned our attention to the situation when kinase activators are present. Existing eIF2 kinases operate in two fundamentally different modes: their activating signal can either arise from the translational machinery itself, or from pathways unconnected to translation. Examples for the first case include Gcn2 which is activated when the consumption of charged tRNAs by translation exceeds the capacity of the tRNA synthetases to regenerate them, and PERK, which is activated when protein synthesis overwhelms the folding capacity of the ER. In these cases, regulation of the translational machinery is connected to a translational output in a classic feedback loop. Similar feedback loops have previously been analysed in other translational control pathways (Betney et al., 2012; de Silva et al., 2010), where feedback properties were found to contribute strongly to the overall dynamic behaviour of the pathway. Examples for the non-feedback mode include PKR, which is activated by viral RNA i.e. not by a product of the translational machinery.

It should be noted that in our analyses we consider modes of regulation where inactive kinase is activated by an activating molecule, which is the case for Gcn2 and PKR. Some eIF2 kinases are regulated in the opposite fashion, ie they are active in the apo-form but are inhibited by inhibiting molecules (such as heme in the case of HRI). Both the addition of an activator or the removal of an inhibitor cause fractional changes in the abundance of active kinase, and our analyses can be understood to illustrate either mode of regulation.

Because non-feedback regulation is the simpler case, we start our analyses with this scenario. For this purpose, we add a species KA (kinase activator) to the model that interacts with the eIF2 kinase with a macromolecular equilibrium binding constant of 10 µM to form an active kinase complex, which is then competent to phosphorylate eIF2.

If we allow the model to run at equilibrium and then raise the concentration of KA, we observe that the translation rate drops to zero over time. The rate of response is concentration dependent, with a lower threshold for the response time (arbitrarily defined here as the time after which translation has dropped by 99%) between two and three minutes (figure 6A). The exact details of the response curve are dependent on the exact rate parameters chosen for kinase activation and eIF2 phosphorylation, but the observed response time is close to the behaviour observed in yeast and mammalian cells.

To model feedback regulation by kinases which rely on activation via translation products, we introduced two new reactions (R12 and R13 in figure 1) into the model which mimic the production of a kinase activator like uncharged tRNA by the translational machinery, and the removal of this activator from the system (representing eg re-charging of uncharged tRNAs by the tRNA synthetases). The behaviour of the system is then principally determined by the ratio of production to removal of the kinase activator: for very low ratios, the system operates essentially as it does in the absence of kinase activator (the top line in the

graph in figure 6B represents a system producing kinase activator at 1/1000th of its rate of removal, and has a steady state indistinguishable from a model running in the absence of kinase activator). For higher ratios, the system very quickly becomes strongly responsive to the production of kinase activator. Under the parameter combinations shown in figure 6, this happens even when the rate of production of KA is much lower than the rate of removal: this is because under steady state conditions, some free tRNA accumulates and is stabilised by forming a complex with the kinase even at low KA production and high removal rates, and this is sufficient to activate eIF2 phosphorylation. Exactly how responsive the system is depends on a number of parameters including the ratio of the rate constants with which the kinase activator interacts with the kinase activator removal system and with the kinase (eg, the association rates of tRNAs with tRNA synthetases and Gcn2), the stability of the kinase:activator complex, and the ratio of phosphorylation and dephosphorylation rates for eIF2. One of the consequences of the strong responsiveness of our model to production of kinase activator is that there is only a very narrow window of parameter combinations in which the system adopts a non-zero steady state: even for low rates of production of kinase activator, the system tends towards a zero translation rate, albeit approaching this rate over very different time scales depending on the rate with which kinase activator is produced.

The very strong sensitivity to kinase activity in both the fed-back and non fed-back modes may be caused by the high molar excess of eIF2 over eIF2B (Singh et al., 2007; von der Haar and McCarthy, 2002), which means that eIF2B can be inhibited even when eIF2 is only partially phosphorylated. It is interesting to consider in how far these observed features of our model reflect the real world behaviour of eIF2-dependent translational control. Real-world systems contain a number of control elements that are absent from our model. For example, Gcn2 itself can be phosphorylated by TORC1, and this phosphorylation prevents activation of Gcn2 kinase activity (Cherkasova and Hinnebusch, 2003). TORC1 activity also has a stimulating effect on translational activity. In consequence, when high translational activity is required, the sensitive system would be prevented from being inappropriately activated eg by low levels of tRNAs. Similarly, PKR can be inhibited by trans-acting modulators like $p58^{IPK}$ (Barber et al., 1994), which could similarly be used to attenuate the response to activation of the kinase. If the strong responsiveness our model predicts is indeed a real-world feature of eIF2-mediated translational control, this could explain why additional regulators evolved for these kinases, and the combination of strong response and trans-acting modulators would ensure both high robustness and high sensitivity of translational control.

Conclusions

Our computational investigation into robustness determining features of translational regulation impinging on eIF2 formulates a number of experimentally testable hypotheses.

The model recapitulates biological control in a number of aspects. The model can reach a steady state translational activity at levels very similar to a well-studied *in vivo* system (yeast), upon activation of the eIF2 kinase translation ceases on a time-sale of minutes, and both of these properties are robust with

respect to parameter choices. We find indications of strong robustness using different analysis approaches, namely explicit parameter variation and structured singular value analyses. This finding of strong robustness is validated by experimental observations that translation *in vivo* can operate despite relatively severe parameter perturbations resulting eg from mutations in eIF2 and eIF2B (Asano et al., 1999; Richardson et al., 2004).

Our further analyses based on model derivatives where dynamics of individual species are constrained indicate that this strong robustness results from distributed model features, and cannot be traced to the behaviour of a single individual species. However, some species' dynamics contribute more to the robustness of the system than others. A strongly contributing species in this respect is the eIF2:eIF2B:eIF5 complex which, although our analyses predict it to be non-essential for the basic operability of the system (figure 5), show the strongest changes in robustness when its dynamics are constrained (figure 4). Interestingly, Jennings *et al.* very recently characterised an eIF2 mutant that prevents eIF5 from functioning as a GDI (Jennings et al., 2016) . This mutant allows normal growth rates, but does not allow robust regulation of translational activity under conditions which would normally lead to activation of the Gcn2 kinase. Although this study did not directly evaluate the effect of the eIF2 mutant on the eIF2:eIF2B:eIF5 complex, these findings are consistent with our predictions that normal formation of this complex is important for robust regulation, but not essential for the basic operability of translation.

One of the outcomes from our study is an indication where models of translational control via eIF2 could be improved in future. There is a paucity of rate constants available for formation of the different macromolecular complexes. This introduces a high degree of freedom into the parameter estimation process, which could be reduced if accurate, experimentally measured rates were available. Moreover, new aspects of the modelled pathways are still being uncovered, such a the recent discovery of a "fail-safe" mechanism by which eIF2 phosphorylation potentiates translational response to eIF2 kinase activation (Jennings et al., 2017). Considering these new findings in model-based analyses will require introducing new reactions and rate-constants, which will only be feasible if the need for parameter fitting can be reduced for existing parameters.

Given the strong sensitivity of our current model to kinase activation, it is likely that additional regulatory layers such as the priming of GCN2 by TOR or the regulation of PKR by trans-acting cellular regulators like $p58^{IPK}$ could strongly modulate the dynamics with which translation responds to regulatory input. The inclusion of such regulation in the model would clearly be desirable, although it is likely that this would introduce too many degrees of freedom in simple, ODE-based models as the majority of these interactions are dynamically almost completely uncharacterised. Qualitative approaches such as Petri-Net based models (Chaouiya, 2007) may enable the analysis of such wider regulatory networks without explicitly considering rate constants.

Methods

Model simulations

The full ODE system representing the model (including R12 and R13) is given in supplementary file 1. For simulations, this model was run using the modified Rosenbrock solver from Matlab (ode23 (Shampine and Reichelt, 1997)).

Levenberg-Marquardt implementation

The rate constants of the model have been estimated using the Levenberg-Marquardt (LM) algorithm (Marquardt, 1963) . In order to develop a naturally behaving mathematical model, the rate constants are optimised using the LM algorithm integrated with pathway characteristics such as positivity and robustness analysis.

Using the LM algorithm alone to parameterise computational models may result in uncertain combinations of parameter values, which may not follow experimental observations appropriately. Therefore, to overcome the limitation of parameter uncertainty, we integrated the robustness characteristics of the general translation rate (Y_1) to parameter changes within the LM algorithm. The integrated parameterisation process used in this work is discussed below. Note that for simplicity the concentration of species considered in the eIF2-dependent translational regulation model are denoted by Y (a conversion from Y notation to standard molecular biology notation is given in table 3).

In order to quantify the changes in general translation rate due to variation in the rate constant vector *k*, the following equation is used.

$\xi_1 = \lvert Y_{1D} - Y_1(Y_i(0), k_i, t)\rvert$	(1)

where, ξ_1 is an absolute error between *in-vitro* and *in-silico* experimental values, Y_{1D} is the *in-vitro* experimental data value of the general translation rate in a yeast cell, $Y_1(Y(0),k, t)$ is the *in-silico* experimental value of the general translation rate obtained after solving the ODEs using the modified Rosenbrock solver with $Y(0)$ and k initial conditions. After obtaining different combinations of parameter values giving $\xi_2 \equiv 0$, the value for each combination of *k* is perturbed +/-50% from the original value and the error ξ_2 with respect to Y_{1D} is recorded. The average value of normalised absolute error ξ_2 can be determined from (2),

X	(2)

where, *T* is the evaluation time and Δk is equal to +/-50% of the original *k* value. The purpose of perturbing the rate constants is to analyse the robustness of general translation rate. Hence a lower value of ξ_2 defines high robustness against internal parametric changes.

Note that, to cope with the limitation that concentration values of most of the species/complexes are unknown, we have opted for a random selection approach which adopts a random value of the initial concentration that should lie within yeast molecular concentration. Typically, in yeast cells the molecular concentrations lie approximately between 10nM-10µM. Hence, the initial concentration of remaining

species/complexes are randomly varied in a bounded limit of [10^{-3},10] µM in a way that the target constraints can be achieved (refer to the subsection on model implementation and parameterisation).

Model linearisation

In control theory, the non-linear model can be linearised around an equilibrium point to investigate some of its properties such as robust stability etc. Linearisation simplifies the non-linear interaction of the species, so that the individual effect of the rate constants can be investigated. There are some limitations of the linear approximation of non-linear systems, that is the linear system is an approximation that is only valid across small regions around equilibrium point. Therefore the approximate linear system accurately predicts the local behaviour of the non-linear systems instead of global.

A generalised form of the non-linear mathematical model given in supplementary file 1 (excluding R12 and R13) can be defined as follows:

$$\dot{Y}(t) = \acute{f}(Y(t), k) \quad (3)$$

where, *Y* is the non-negative concentration of the species, *t* is the evaluation time and *k* is a rate constant vector. In order to find the equilibrium point of a model or a steady state value of all the species, eq. 3 is to be solved by equating it to zero. Note that, substituting *f*(*Y*(*t*); *k*) to zero implies no change in the state of all species as time progresses that is all species have attained a steady state. Solving the equation results into one of the biologically feasible equilibrium point Y^{eq} displayed in table 3.

Prior to investigating the role of uncharged tRNA (Y_{13}) on other species, it is beneficial to eliminate the dynamics of Y_{13} from the original non-linear model. The investigation has revealed that Y_{13} has attained the quasi steady state or constant steady state value for varying initial concentrations (Segel and Slemrod, 1989). Hence, substituting $Y_{13} = 0$ makes no difference in the behaviour of modified non-linear system compared to the original non-linear system. Performing this task gives freedom to consider Y_{13} as an applied input *u* and helps to analyse the direct impact of uncharged tRNA on translation rate. The state space model of the modified non-linear model can be defined as follows:

$$\begin{aligned} \acute{Y}(t) &= Y(Y(t), k) + B\big(Y(t)\big)u \\ Z(t) &= Y_1(t) \end{aligned} \quad (4)$$

where vector $B\big(Y(t)\big) = \big[00000000 - k_{8f}Y_9 k_{8f}Y_9 000\big]^T$, vector $Y(t) = [Y_1 Y_2 \cdots Y_{12} Y_{14}]^T$, vector $k = \big[k_1 k_{2f} k_{2r} \cdots k_{12}\big]$, $u = Y_{13}$ and $Z(t)$ is the output signal or translation rate. The state space representation of an approximate LTI model of a modified non-linear system around the equilibrium point can be re-written in the form:

$$\begin{aligned} \acute{Y} &= AY + Bu \\ Z &= DY \end{aligned} \quad (5)$$

where *A* is a constant Jacobian matrix, *B* and *D* are the constant input and output vectors respectively given as:

$$B = [00000000 - 4.331 \times 10^{-11} 4.331 \times 10^{-11} 000]$$

$$D = [1000000000000]$$

Note that the matrix *A* of dimensions 13×13 is a function of the equilibrium point and rate constant vector *k*. The Jacobian matrix *A* represents the behaviour of the overall biological system around an equilibrium point (Y^{eq}).

Mu (μ) analysis

Within control engineering, robust stability is a measure of how much uncertainty of a specific parameter the feedback loop can tolerate before becoming unstable. In order to determine the extreme limits to which rate constants of the model can vary without impacting the robustness of the system, we conducted a structured singular value (μ) analysis (Fan et al., 1991; Kim et al., 2006).

$$\mu = \frac{1}{\min_{\Delta}\{\acute{\sigma}(\Delta) \vee det(I - M(s)\Delta) = 0 for \Delta \in B_{\Delta}\}} \quad (6)$$

where $\acute{\sigma}$ represents the maximum singular value, *M*(s) denotes the transfer function of the system and B_{Δ} represents a set of uncertainties **Δ**. From the above equation it is clear that the principle at which μ-analysis works is finding the smallest value of $\acute{\sigma}(\Delta)$ that can make $I - M(s)\Delta$ singular, and when there is no **Δ** such that $det(I - M(s)\Delta) = 0$ then $\mu = 0$.

Note that, μ-analysis is a deterministic measure which computes a level of uncertainty at which the model is guaranteed to produce desirable results. One of the advantage of opting μ-analysis is that it provides information on robustness of the system when the parameters of the system encounters simultaneous perturbation (Kim et al., 2006). This particular scenario resembles the actual behaviour of robust biological systems because under environmental disturbances the parameters of the biological systems can fluctuate simultaneously without impacting the behaviour of the system. So higher value of upper bound of μ^{-1} is desirable for robust biological systems.

In order to evaluate the parametric perturbation limits of a biological system, the equivalent linearised biological system needs to be connected through a feedback control loop to a matrix of uncertain parameters **Δ**. The robustness analysis of a biological system using μ requires the system to be represented in a stable linear time invariant (LTI) form.

To analyse the robustness of the system, a parametric uncertainty matrix block **Δ** is introduced into the LTI biological system represented in (5). Note that, the parametric uncertainty matrix block is only consisting of diagonal entries of the individual parameters. Thus, obtaining upper bound of μ-analysis it can be guaranteed that the system is robust provided that no single parameter differs more than upper bound of μ^{-1}×100% from its nominal value. Figure 7 represents the biological system *M*(*s*) connected through a closed feedback loop which can be destabilised from the smallest possible uncertainty **Δ**. Note that, $\Delta = diag\left[\delta_{k1}\delta_{k2f}\delta_{k2r}\cdots\delta_{k12}\right]$ and *M*(*s*) is the transfer function of the LTI model defined as:

$M(s) = D(sI - A_i)^{-1}B_i$	(7)

Now, introducing **Δ** into the system changes the rate constant *k* to $k(1+\delta_k)$. The state space representation of the perturbed system is as follows:

$\delta\acute{Y} = a\delta Y + B_0\Delta Y$ $Y = D_0\delta Y$	(8)

Note that the dimensions of the constant matrices B_0 and D_0 are 13×20 and 20×13 respectively. The matrices B_0 and D_0 for the perturbed LTI system are defined below.

$B_0(i,j) = 1$	(9)

for (*i,j*) equals (1,11), (2,1), (2,3), (2,7), (3,3), (3,9), (3,10), (3,17), (4,2), (4,5), (5,4), (5,6), (6,4), (6,8), (7,6), (7,9), (7,15), (7,18), (8,10), (9,13), (10,12), (10,15), (10,19), (11,17), (11,19), (12,16), and (13,14).

$B_0(i,j) = -1$	(10)

for (*i,j*) equals (1,1), (1,20), (2,2), (2,6), (3,2), (3,8), (3,16), (4,3), (4,4), (5,5), (5,7), (5,11), (6,5), (6,9), (6,10), (7,7), (7,8), (7,14), (8,11), (9,12), (10,13), (10,14), (11,16), (11,18), (12,17), (13,15), and (13,19). The remaining elements of $B_0(i,j) = 0$. On the other hand, all the elements of matrix D_0 are zero except:

$D_0(1,1) = k_1,\ D_0(2,2) = k_{4f}Y_3^{eq},\ D_0(2,3) = k_{4f}Y_2^{eq}, D_0(3,4) = k_{4r}, D_0(4,4) = k_{5f}, D_0(5,5) = k_{5r}Y_6^{eq}, D_0(5,6) = k_{5r}Y_5^{eq}, D_0(6,2) = k_{2f}, D_0(7,5) = k_{2r}Y_7^{eq}, D_0(7,7) = k_{2r}Y_5^{eq}, D_0(8,3) = k_{3f}Y_7^{eq}, D_0(8,7) = k_{3f}Y_3^{eq}, D_0(9,6) = k_{3r}, D_0(10,6) = k_6, D_0(11,5) = k_7Y_8^{eq}, D_0(11,8) = k_7Y_5^{eq}, D_0(12,9) = k_{8f}Y_{13}^{eq}, D_0(13,10) = k_{8r}, D_0(14,7) = k_{9af}Y_{10}^{eq}, D_0(14,10) = k_{9af}Y_7^{eq}, D_0(15,13) = k_{9ar}, D_0(16,3) = k_{10f}Y_{11}^{eq}, D_0(16,11) = k_{10f}Y_3^{eq}, D_0(17,12) = k_{10r}, D_0(18,11) = k_{11}, D_0(19,13) = k_{9b}, D_0(20,1) = k_{12}$	(11)

Analysing system (8) using the Matlab μ-analysis tool within the Robust Control Toolbox from Mathworks, will give the value at which the rate constant can be perturbed individually without impacting the structured robustness of the system.

References

Asano, K., Krishnamoorthy, T., Phan, L., Pavitt, G.D., Hinnebusch, A.G., 1999. Conserved bipartite motifs in yeast eIF5 and eIF2Bepsilon , GTPase-activating and GDP-GTP exchange factors in translation initiation, mediate binding to their common substrate eIF2. EMBO J. 18, 1673–1688. https://doi.org/10.1093/emboj/18.6.1673

Barber, G.N., Thompson, S., Lee, T.A.E.G., Strom, T.E.D., Jagust, R., Darveau, A., Katze, M.G., 1994. The 58-kilodalton inhibitor of the interferon-induced double-stranded RNA-activated protein kinase is a tetratricopeptide repeat

protein with oncogenic properties. Proc. Natl. Acad. Sci. USA 91, 4278–4282.

Betney, R., de Silva, E., Mertens, C., Knox, Y., Krishnan, J., Stansfield, I., 2012. Regulation of release factor expression using a translational negative feedback loop: a systems analysis. RNA 18, 2320–2334. https://doi.org/10.1261/rna.035113.112

Chaouiya, C., 2007. Petri net modelling of biological networks. Brief. Bioinform. 8, 210–219. https://doi.org/10.1093/bib/bbm029

Chen, J.-J., 2006. Regulation of protein synthesis by the heme-regulated eIF2 kinase: relevance to anemias. Blood 109, 2693–9. https://doi.org/10.1182/blood-2006-08-041830

Cherkasova, V.A., Hinnebusch, A.G., 2003. Translational control by TOR and TAP42 through dephosphorylation of eIF2alpha kinase GCN2. Genes Dev. 17, 859–872. https://doi.org/10.1101/gad.1069003

Chu, D., Barnes, D.J., Von Der Haar, T., 2011. The role of tRNA and ribosome competition in coupling the expression of different mRNAs in Saccharomyces cerevisiae. Nucleic Acids Res. 39, 6705–6714. https://doi.org/10.1093/nar/gkr300

Chu, D., Kazana, E., Bellanger, N., Singh, T., Tuite, M.F., von der Haar, T., 2014. Translation elongation can control translation initiation on eukaryotic mRNAs. EMBO J. 33, 21–34. https://doi.org/10.1002/embj.201385651

de Silva, E., Krishnan, J., Betney, R., Stansfield, I., 2010. A mathematical modelling framework for elucidating the role of feedback control in translation termination. J. Theor. Biol. 264, 808–21. https://doi.org/10.1016/j.jtbi.2010.01.015

Dey, M., Trieselmann, B., Locke, E.G., Lu, J., Cao, C., Dar, A.C., Krishnamoorthy, T., Dong, J., Sicheri, F., Dever, T.E., 2005. PKR and GCN2 Kinases and Guanine Nucleotide Exchange Factor Eukaryotic Translation Initiation Factor 2B (eIF2B) Recognize Overlapping Surfaces on eIF2. Mol. Cell. Biol. 25, 3063–3075. https://doi.org/10.1128/MCB.25.8.3063-3075.2005

Dimelow, R.J., Wilkinson, S.J., 2009. Control of translation initiation: a model-based analysis from limited experimental data. J. R. Soc. Interface 6, 51–61. https://doi.org/10.1098/rsif.2008.0221

Dong, J., Qiu, H., Garcia-Barrio, M., Anderson, J., Hinnebusch, a G., 2000. Uncharged tRNA activates GCN2 by displacing the protein kinase moiety from a bipartite tRNA-binding domain. Mol. Cell 6, 269–279. https://doi.org/10.1016/S1097-2765(00)00028-9

Donnelly, N., Gorman, A.M., Gupta, S., Samali, A., 2013. The eIF2α kinases: Their structures and functions. Cell. Mol. Life Sci. 70, 3493–3511. https://doi.org/10.1007/s00018-012-1252-6

El-Haroun, E.R., Bureau, D.P., Cant, J.P., 2010. A mechanistic model of nutritional control of protein synthesis in animal tissues. J. Theor. Biol. 262, 361–9. https://doi.org/10.1016/j.jtbi.2009.09.034

Fan, M.K.H., Tits, A.L., Doyle, J.C., 1991. Robustness in the presence of mixed parametric uncertainty and unmodeled dynamics. IEEE Trans. Automat. Contr. 36, 25–38. https://doi.org/10.1109/9.62265

Firczuk, H., Kannambath, S., Pahle, J., Claydon, A., Beynon, R., Duncan, J., Westerhoff, H., Mendes, P., McCarthy, J.E., 2013. An in vivo control map for the eukaryotic mRNA translation machinery. Mol. Syst. Biol. 9, 1–13. https://doi.org/10.1038/msb.2012.73

Fjeld, C.C., Denu, J.M., 1999. Kinetic analysis of human serine/threonine protein phosphatase 2Calpha. J. Biol. Chem. 274, 20336–20343.

Gebauer, F., Hentze, M.W., 2004. Molecular mechanisms of translational control. Nat. Rev. Mol. Cell Biol. 5, 827–835. https://doi.org/10.1038/nrm1488

Hershey, J.W.B., Sonenberg, N., Mathews, M. (Eds.), 2007. Translational Control in Biology and Medicine, 3rd Ed. ed. Cold Spring Harbor Laboratory Press, Cold Spring Harbor, New York.

Hinnebusch, A.G., 2014. The scanning mechanism of eukaryotic translation initiation. Annu. Rev. Biochem. 83, 779–812. https://doi.org/10.1146/annurev-biochem-060713-035802

Jedlicka, P., Panniers, R., 1991. Mechanism of activation of protein synthesis initiation in mitogen- stimulated T lymphocytes. J Biol Chem 266, 15663–15669.

Jennings, M.D., Kershaw, C.J., Adomavicius, T., Pavitt, G.D., 2017. Fail-safe control of translation initiation by dissociation of eIF2α phosphorylated ternary complexes. Elife 6, e24542. https://doi.org/10.7554/eLife.24542

Jennings, M.D., Kershaw, C.J., White, C., Hoyle, D., Richardson, J.P., Costello, J.L., Donaldson, I.J., Zhou, Y., Pavitt, G.D., 2016. eIF2β is critical for eIF5-mediated GDP-dissociation inhibitor activity and translational control. Nucleic Acids Res. gkw657. https://doi.org/10.1093/nar/gkw657

Jennings, M.D., Pavitt, G.D., 2010. eIF5 has GDI activity necessary for translational control by eIF2 phosphorylation. Nature 465, 378–381. https://doi.org/10.1038/nature09003.eIF5

Jennings, M.D., Zhou, Y., Mohammad-Qureshi, S.S., Bennett, D., Pavitt, G.D., 2013. eIF2B promotes eIF5 dissociation from eIF2*GDP to facilitate guanine nucleotide exchange for translation initiation. Genes Dev. 27, 2696–2707. https://doi.org/10.1101/gad.231514.113

Kim, J., Bates, D.G., Postlethwaite, I., Ma, L., Iglesias, P.A., 2006. Robustness analysis of biochemical network models. IEE Proc. - Syst. Biol. 153, 96. https://doi.org/10.1049/ip-syb:20050024

Manchester, K.L., 1990. Kinetic modelling of the effect of alpha subunit phosphorylation on the activity of the protein synthesis initiation factor eIF-2. Biochem. Int. 22, 623–533.

Marquardt, D.W., 1963. An Algorithm for Least-Squares Estimation of Nonlinear Parameters. J. Soc. Ind. Appl. Math. 11, 431–441. https://doi.org/10.1137/0111030

Matts, R., Levin, D., London, I., 1983. Effect of phosphorylation of the alpha-subunit of eukaryotic initiation factor 2 on the function of reversing factor in the initiation of protein synthesis. Proc. Natl. Acad. Sci. U. S. A. 80, 2559–2563.

Mohammed-Qureshi, S.S., Jennings, M.D., Pavitt, G.D., 2008. Clues to the mechanism of action of eIF2B, the guanine-nucleotide-exchange factor for translation initiation. Biochem. Soc. Trans. 36, 658–664.

Moré, J.J., 1978. The Levenberg-Marquardt algorithm: Implementation and theory, in: Watson, G.A. (Ed.), Numerical Analysis: Proceedings of the Biennial Conference Held at Dundee, June 28–July 1, 1977. Springer Berlin Heidelberg, Berlin, Heidelberg, pp. 105–116. https://doi.org/10.1007/BFb0067700

Nika, J., Yang, W., Pavitt, G.D., Hinnebusch, A.G., Hannig, E.M., 2000. Purification and Kinetic Analysis of eIF2B from Saccharomyces cerevisiae. J. Biol. Chem. 275, 26011–26017. https://doi.org/10.1074/jbc.M003718200

Price, N.T., Welsh, G.I., Proud, C.G., 1991. Phosphorylation of only serine-51 in protein synthesis initiation factor-2 is associated with inhibition of peptide-chain initiation in reticulocyte lysates. Biochem. Biophys. Res. Commun. 176, 993–999. https://doi.org/10.1016/0006-291X(91)90380-P

Richardson, J.P., Mohammad, S.S., Pavitt, G.D., 2004. Mutations causing childhood ataxia with central nervous system hypomyelination reduce eukaryotic initiation factor 2B complex formation and activity. Mol. Cell. Biol. 24, 2352–2363.

Segel, L.A., Slemrod, M., 1989. The Quasi-Steady-State Assumption: A Case Study in Perturbation. SIAM Rev. 31, 446–477. https://doi.org/10.1137/1031091

Shampine, L.F., Reichelt, M.W., 1997. The MATLAB ODE Suite. SIAM J. Sci. Comput. 18, 1–22.

https://doi.org/10.1137/S1064827594276424

Singh, C.R., Lee, B., Udagawa, T., Mohammad-Qureshi, S.S., Yamamoto, Y., Pavitt, G.D., Asano, K., 2006. An eIF5/eIF2 complex antagonizes guanine nucleotide exchange by eIF2B during translation initiation. EMBO J. 25, 4537–4546. https://doi.org/10.1038/sj.emboj.7601339

Singh, C.R., Udagawa, T., Lee, B., Wassink, S., He, H., Yamamoto, Y., Anderson, J.T., Pavitt, G.D., Asano, K., 2007. Change in Nutritional Status Modulates the Abundance of Critical Pre-initiation Intermediate Complexes During Translation Initiation in Vivo. J. Mol. Biol. 370, 315–330. https://doi.org/10.1016/j.jmb.2007.04.034

Spirin, A.S., 2009. How Does a Scanning Ribosomal Particle Move along the 5′-Untranslated Region of Eukaryotic mRNA? Brownian Ratchet Model. Biochemistry 48, 10688–10692.

von der Haar, T., 2008. A quantitative estimation of the global translational activity in logarithmically growing yeast cells. BMC Syst. Biol. 2, 87. https://doi.org/10.1186/1752-0509-2-87

von der Haar, T., McCarthy, J.E.G., 2002. Intracellular translation initiation factor levels in Saccharomyces cerevisiae and their role in cap-complex function. Mol. Microbiol. 46, 531–544. https://doi.org/10.1046/j.1365-2958.2002.03172.x

Wortham, N.C., Proud, C.G., 2015. eIF2B: recent structural and functional insights into a key regulator of translation. Biochem. Soc. Trans. 43, 1234–40. https://doi.org/10.1042/BST20150164

You, T., Coghill, G.M., Brown, A.J.P., 2010. A quantitative model for mRNA translation in Saccharomyces cerevisiae. Yeast 27, 785–800. https://doi.org/10.1002/yea

Zhan, K., Narasimhan, J., Wek, R.C., 2004. Differential Activation of eIF2 Kinases in Response to Cellular Stresses in Schizosaccharomyces pombe. Genetics 1875, 1867–1875. https://doi.org/10.1534/genetics.104.031443

Table 1. Literature values used for model parameterisation.

Parameter	Value[a]	References
Translation	13,000 proteins per second	(von der Haar, 2008)
total cellular eIF2	18 µM	(Singh et al., 2007; von der Haar, 2008)
Total cellular eIF2B	1.8 µM	(Singh et al., 2007; von der Haar, 2008)
Total cellular eIF5	18 µM	(Singh et al., 2007)
Total cellular kinase (Gcn2)	0.09 µM	(Singh et al., 2007)

[a]Where appropriate, intracellular concentrations were calculated from molecule numbers based on a typical haploid yeast cell volume of 27 μm^3 or $2.7x10^{-14}$ litres (von der Haar and McCarthy, 2002) .

Table 2. Steady state rate constants and comparison to literature values.

Rate	Value	Reaction	Reported value
k1	1.77 s^{-1}	(translation)	A k1 value of **1.78 s^{-1}** is equivalent to a flux of ~13,000 translation events per second in the steady state (von der Haar, 2008)
k2f	7.59 s^{-1}	eIF5 release from 5:2:GDP	No data
k2r	0.91 $M^{-1}s^{-1}$		
k3f	6×10^{7} $M^{-1}s^{-1}$	2B:2:GDP complex formation	K_M of **0.7-1.2x10^{-8}** at 0˚C (Nika et al., 2000) vs. **2.5e^{-6}** calc. from (k6+k3r)/k3f
k3r	150 s^{-1}		
k4f	1.0 $M^{-1}s^{-1}$	5:2:2B:GDP complex formation	no data
k4r	0.72 s^{-1}		
k5f	0.36 s^{-1}	eIF5 release from 5:2:2B:GDP	no data
k5r	$1.6\text{x}10^{4}$ $M^{-1}s^{-1}$		
k6	0.72 s^{-1}	GDP release from 2:2B:GDP	**0.7-7 sec^{-1}** (Nika et al., 2000)
k7	$7.4\text{x}10^{4}$ $M^{-1}s^{-1}$	(translation)	A k7 value of **7.3x10^{4} M^{-1} s^{-1}** is equivalent to a flux of ~13,000 translation events per second in the steady state (von der Haar, 2008)
k8f	1×10^{6} $M^{-1}s^{-1}$	GCN2:tRNA complex formation	no data
k8r	203 s^{-1}		
k9af	1×10^{9} $M^{-1}s^{-1}$	phosphorylation reaction	K_M of **10^{-5} to 10^{-6} M** for human PKR (Dey et al., 2005) vs **1.0x10^{-4} M** calculated from (k9ar + k9b)/k9af
k9ar	167 s^{-1}		
k9b	1×10^{5} s^{-1}		
k10f	1×10^{2} $M^{-1}s^{-1}$	2-P:2B:GDP complex formation	no data
k10r	129 s^{-1}		
k11	1×10^{-4} s^{-1}	phosphatase reaction	**10^{-3} to 10^{-5} sec^{-1}** at 1 µM enzyme for human PP2Cα (Fjeld and Denu, 1999)
k12	1×10^{-8} s^{-1}	(tRNA release from translation)	na
k13	$1\text{x}10^{-2}$ s^{-1}	tRNA recharging	**10^{-2} to 10^{2} sec^{-1}** at 1-10 µM tRS for various yeast enzymes (Chu et al., 2011)

Table 3. Species denominations and equilibrium points for species abundance.

Y_1	translation	4.36×10^{-7} M
Y_2	eIF5:eIF2:GDP	1.19×10^{-7} M
Y_3	eIF2B	7.22×10^{-7} M
Y_4	eIF5:eIF2B:eIF2:GDP	1.78×10^{-7} M
Y_5	eIF5	1.11×10^{-5} M
Y_6	eIF2B:eIF2:GDP	1.07×10^{-6} M
Y_7	eIF2:GDP	3.74×10^{-7} M
Y_8	eIF2:GTP	9.44×10^{-6} M
Y_9	GCN2	4.33×10^{-17} M
Y_{10}	tRNA:GCN2	2.22×10^{-18} M
Y_{11}	eIF2-P	1.61×10^{-12} M
Y_{12}	eIF2-P:eIF2B	4.04×10^{-18} M
Y_{13}	tRNA	1.04×10^{-5} M
Y_{14}	tRNA:GCN2:eIF2	8.23×10^{-21} M

Figure Legends

Figure 1. Graphical presentation of the eIF2-dependent translational regulation model. The model is conceptually divided into a core section which comprises the reactions required for sustaining ongoing translation, and regulatory reactions that can be used to exert regulation on the core section. Regulation can be exerted either in a fed-back mode through reactions 12 and 13, or in a non-fed-back manner if reactions 12 and 13 are removed from the model. Double-headed arrows above the reaction numbers indicate reactions that are modelled via reversible mass-action kinetics. The species indicated are: 2, eIF2; 2-P, phosphorylated eIF2; 2B, eIF2B; 5, eIF5; K, kinase; KA, kinase activator.

Figure 2. Principal behaviour and robustness of the model. A, simulation of the model without kinase activator (KA in figure 1). **B,** simulation with 10 μM KA injected at t = 0 s. Error bars represent the variability of the model as observed in the parameter variation exercise discussed in the text.

Figure 3. Upper bound of the structured singular value μ. The inverse of the peak value determines the maximum value of the perturbation in a single parameter which has no impact on the robust stability of the system.

Figure 4. Bode diagrams for three representative model species. We observe partial tracking of the original and truncated, linearised models for all analysed species across the frequency range. The analysis indicates that eIF2:GDP can be expected to have the smallest effect on the input output behaviour of translational control via eIF2.

Figure 5. Model performance in the absence of redundant pathways leading to eIF2:eIF2B complex formation. When formation of the eIF2:GDP:eIF5:eIF2B intermediate complex is disallowed, the model shows a very similar steady-state in the absence of kinase activator (A) as well as a similar response to the presence of kinase activator (B). When formation of this complex is the only allowed route leading to the guanine nucleotide exchange complex (ie when decay of the eIF2:eIF5 complex into free eIF2:GDP and eIF5 is disallowed), the model does not reach a steady state.

Figure 6. eIF2 kinase-dependent regulation of translation. A, regulation in a non-fed-back model. Upon injection of kinase activator (KA) at t=0, translational activity declines with the rate of decline dependent on the concentration of the activator. The inset graph illustrates the time to reach a 99% reduction in translational activity as a function of KA concentration. B, regulation in a fed-back model. The evolution of the model starting without kinase activator is shown, as function of different production/removal ratios for KA.

645

Figure 7: *M*-Δ configuration of eIF2 pathway for μ analysis.

Highlights for Review

-Mathematical tools from the control engineering domain were applied to analysing a mathematical model of the integrated stress response pathway, a translational control pathway universally conserved in eukaryotes
-Structured singular value analyses predict that switching properties of this pathway are exceptionally robust to intrinsic and extrinsic perturbations, recapitulating experimental observations
-Using model reduction techniques, it is shown that the dynamics of different model species make different contributions to robustness. The strongest contribution comes from a recently discovered supercomplex formed by the translation factors eIF2, eIF5 and eIF2B
-Pathways derived from the core integrated stress response are exist as feedback-controlled and non-feedback-controlled variants. We make predictions about different types of response elicited by these two variants.

4. Figure

Click here to download high resolution image

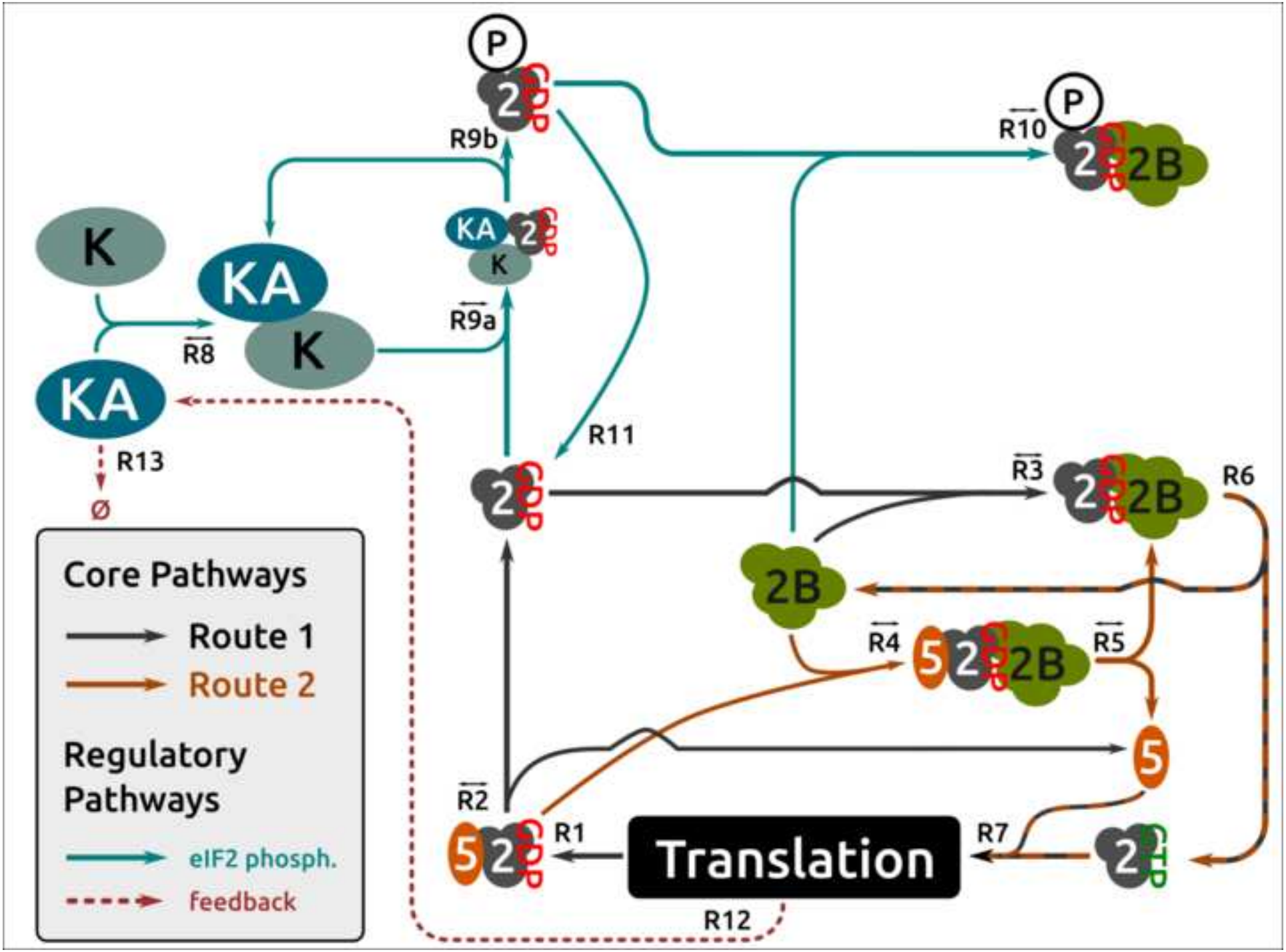

4. Figure

Click here to download high resolution image

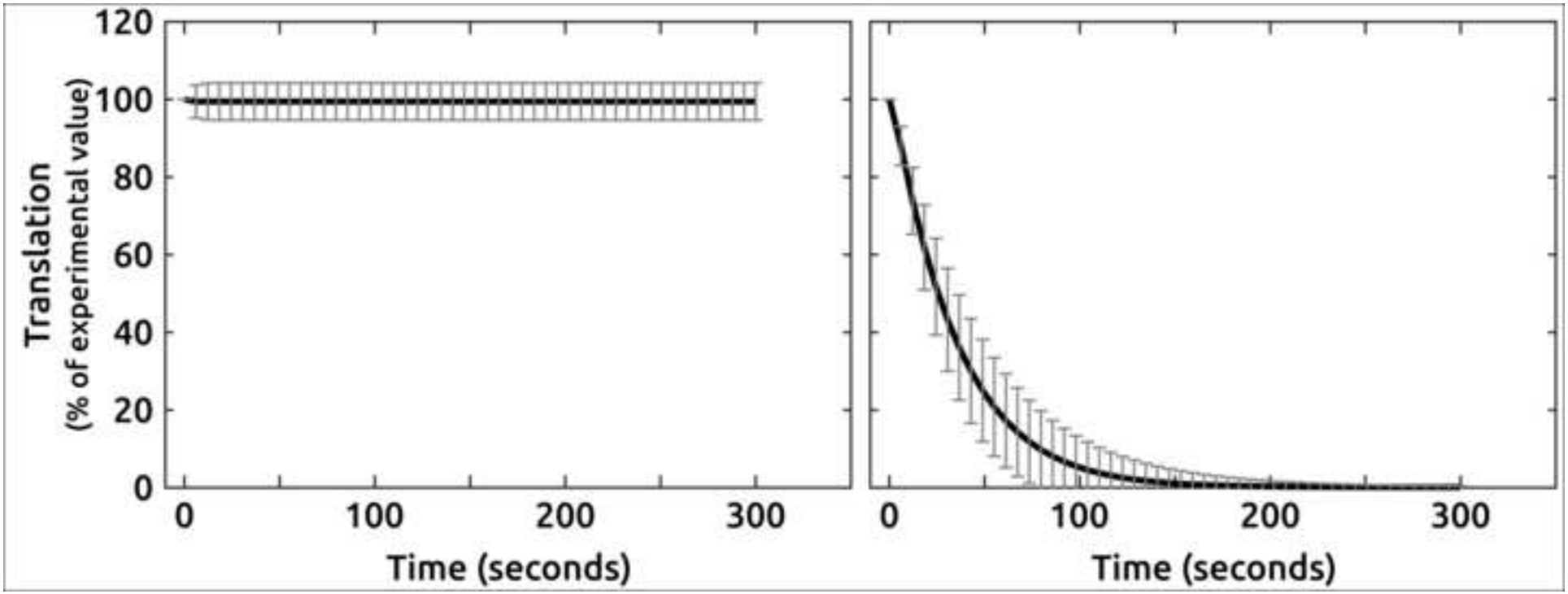

4. Figure

Click here to download high resolution image

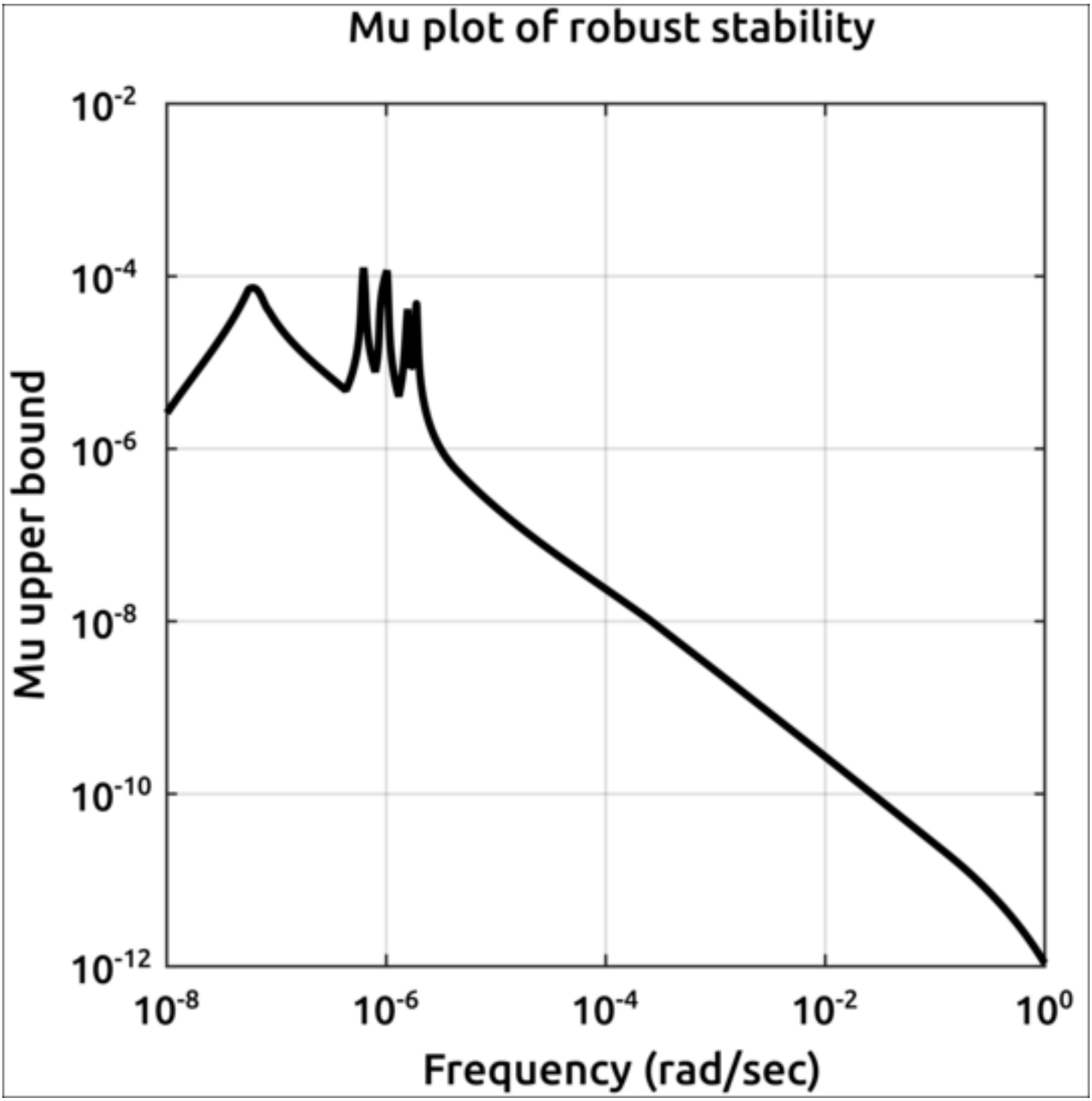

4. Figure

Click here to download high resolution image

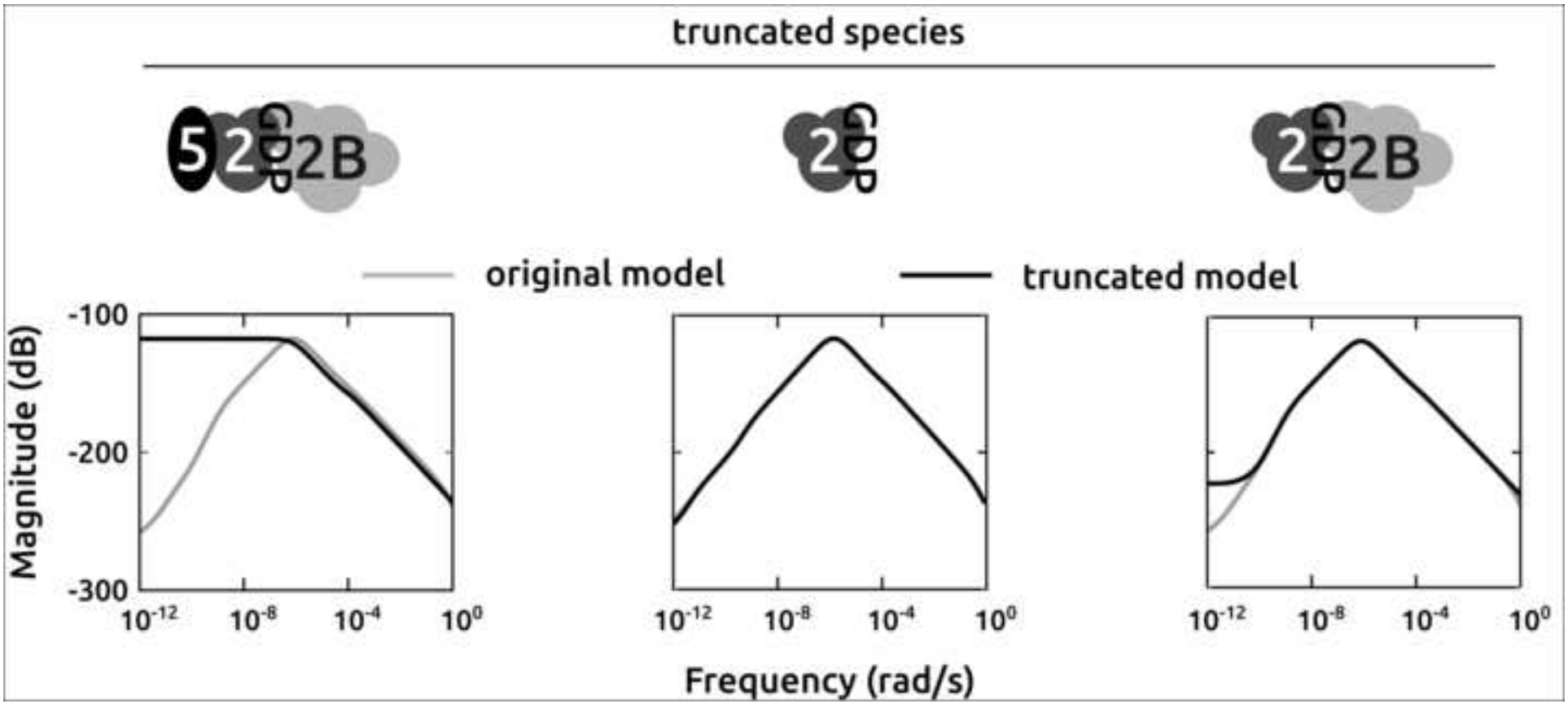

4. Figure

Click here to download high resolution image

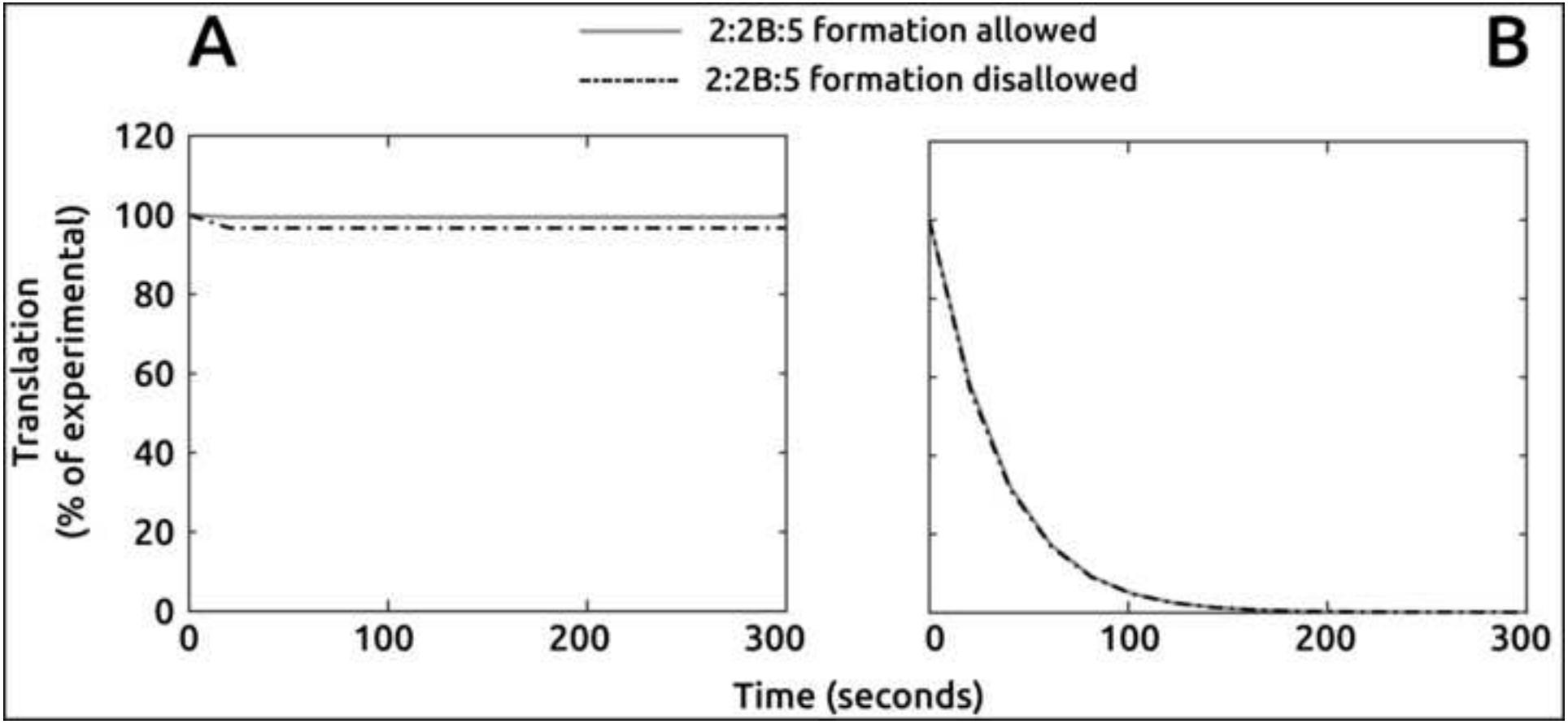

4. Figure

Click here to download high resolution image

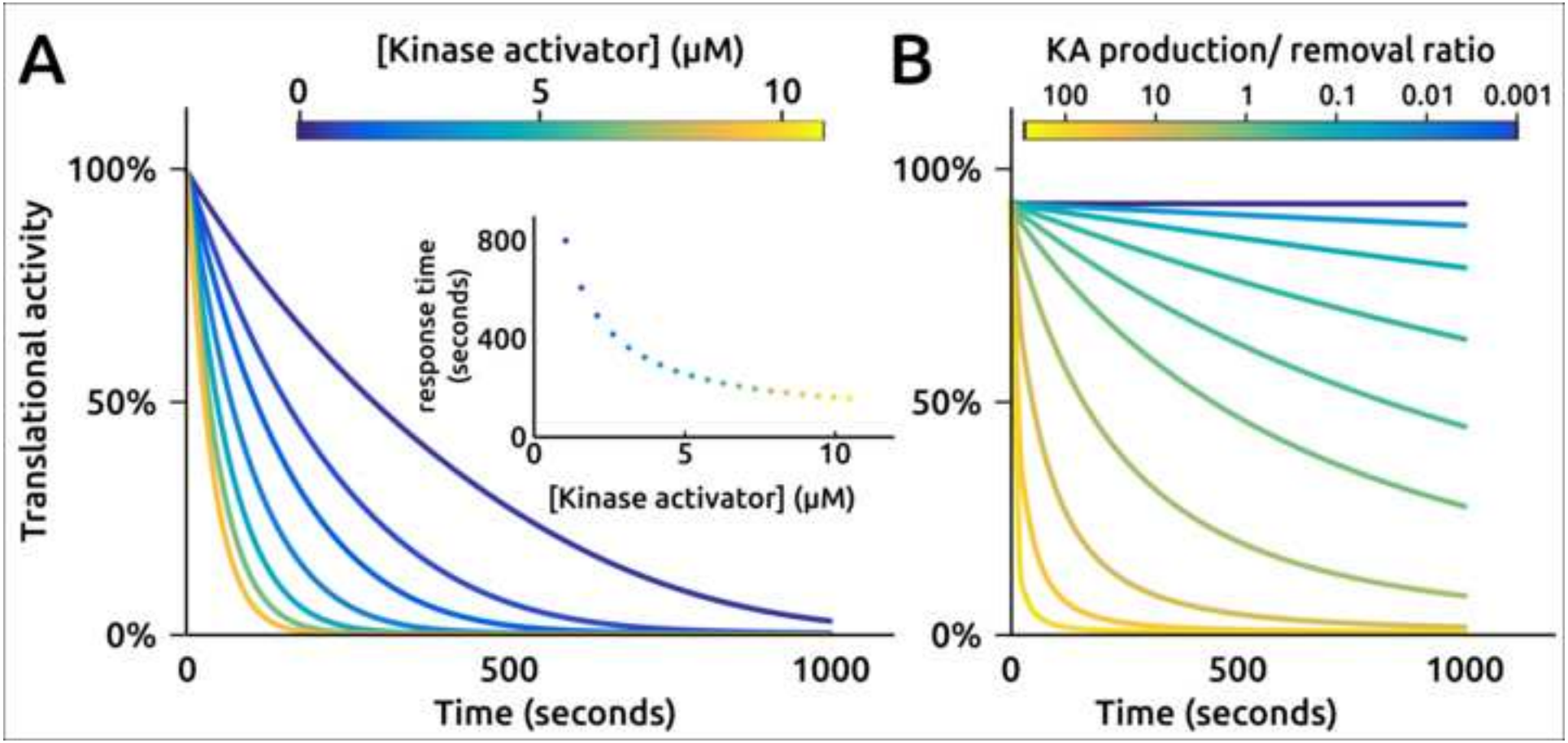

4. Figure

Click here to download high resolution image

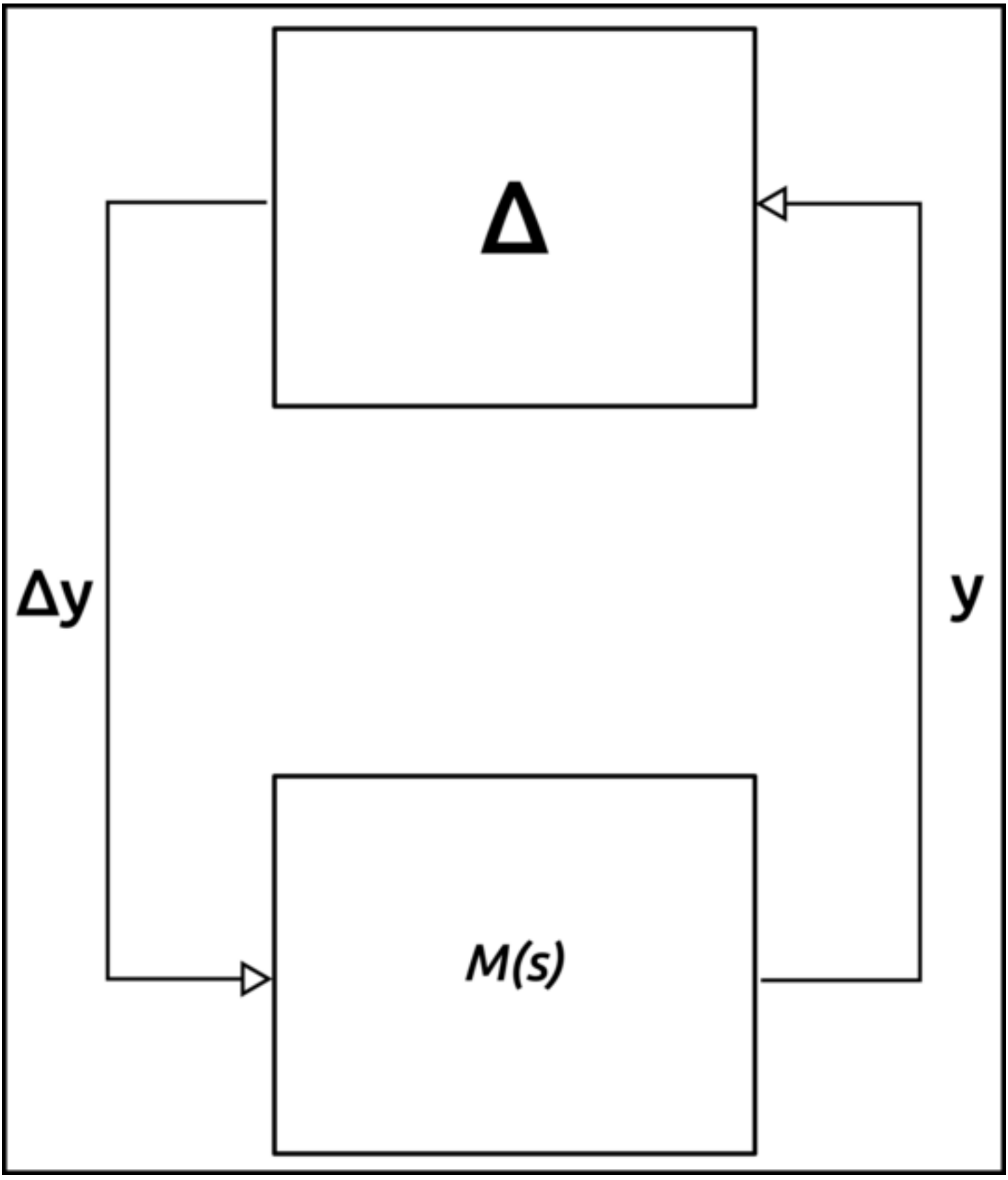

6. Supplementary Material for on-line publication only

Click here to download 6. Supplementary Material for on-line publication only: Farhan Khan et al 2018 Revision ODEs.txt